Comparative Study of Dispersion and Other Losses including Nonlinear Impairments of Different Models of Photonic Crystal Fiber (PCF) by Varying Geometrical Shapes

A thesis submitted in partial fulfillment of the requirements for the degree of Bachelor of Science in Electrical Electronic and Communication Engineering

by

Soheli Noshin Prottasha **Student ID: 201416010**

Neti Nowrin Nilma Ahmed **Student ID: 201416035**

Jinia Afroj **Student ID: 201416039**

Under the Supervision of

Lt. Col. Md. Jahangir Hossain, te, sigs.

Department of Electrical, Electronic and Communication Engineering
Military Institute of Science and Technology (MIST)
Mirpur Cantonment, Dhaka-1216

December, 2017

APPROVAL PAGE

This thesis paper titled **"Comparative Study of Dispersion and Other Losses including Nonlinear Impairments of Different Models of Photonic Crystal Fiber (PCF) by Varying Geometrical Shapes"** is submitted by the group as mentioned below has been accepted as satisfactory and met the required standard in partial fulfillment of the requirement for the degree of B.Sc in Electrical, Electronic and Communication Engineering on December 2017.

Group Members:

Soheli Noshin Prottasha

Neti Nowrin Nilma Ahmed

Jinia Afroj

SUPERVISOR:

Lt. Col. Md. Jahangir Hossain, te, sigs.

Faculty of Electrical and Communication Engineering (EECE)
Military Institute of Science and Technology (MIST)

DECLARATION

It is hereby declared that the work presented in this thesis titled "Comparative Study of Dispersion and Other Losses including Nonlinear Impairments of Different Models of Photonic Crystal Fiber (PCF) by Varying Geometrical Shapes" is an outcome of the study carried out by the author under the supervision of Lt. Col. Md. Jahangir Hossain, te, sigs. It is also declared that neither of this thesis paper nor any part therefore has been submitted anywhere else for the award of any degree, diploma or other qualifications.

AUTHORS:

Soheli Noshin Prottasha
Student ID: 201416010

Neti Nowrin Nilma Ahmed
Student ID: 201416035

Jinia Afroj
Student ID: 201416039

ACKNOWLEDGEMENT

First of all, we would like to thank Allah for giving us the ability to complete this thesis work. We would like to express our utmost gratitude towards our honorable supervisor, Lt. Col. Md. Jahangir Hossain, without whose encouragement and guidance, this thesis would have never been completed. We are very grateful for his continuous instructions and encouragement, valuable discussions and careful review during the entire duration of the research. His thoughtful analyses and firm supervision have provided us with the right direction towards our goal. We have learned many valuable concepts of Optical fiber Communication from him throughout our study, which we tried to utilize and develop our analyzing abilities. His constant encouragement gave us the confidence to carry out our work. We would also like to thank all our teachers. They gave the knowledge and directions needed throughout my life. We express our gratitude towards our teachers from Military Institute of Science and Technology (MIST).

Last but not the least; we would like to thank our parents. Their unconditional support made it possible to finish this thesis.

Dhaka

December, 2017

Soheli Noshin Prottasha

Neti Nowrin Nilma Ahmed

Jinia Afroj

ABSTRACT

This thesis paper presents detail analysis of a hexagonal, octagonal, decagonal and hybrid shaped photonic crystal fiber (PCF) with an aim to compare their performance over various parameters of communication. Deliberate study on the constructional design of the PCF models is carried out to find the optical signal guidance mechanisms through it. The COMSOL Multi-Physics 4.4 Simulation Software is used to perform the modal analysis of the designed PCFs. Three conventional PCFs such as H-PCF, O-PCF and D-PCF are constructed with four layered circular air hole rings. The hybrid structure (Hy-PCF) is also made of four air hole rings but consists of elliptical and square air holes along with the circular ones. Pure silica material is used as core-cladding materials. All the properties are analyzed for 0.80-2.00μm wavelengths range. The dispersion profile of the H-PCF is found quite varying whereas the O-PCF and D-PCF have shown zero to negative dispersion with little variation. At 1.55 μm wavelengths, the calculated dispersion for H-PCF, O-PCF and D-PCF are −2.80 ps/nm-km, −8.61 ps/nm-km and−11 ps/nm-km respectively. The Hy-PCF has exhibited more negative dispersion with almost linearly decreasing characteristics against wavelengths. The value is −81.08 ps/nm-km for 1.55 μm wavelengths. A very negligible confinement loss is obtained for H-PCF, O-PCF and D-PCF for a large wavelengths range. At 1.55 μm wavelengths the H-PCF, O-PCF, D-PCF and Hy-PCF have provided 25.42 μm^2, 19.83 μm^2, 15.7 μm^2 and 5.15 μm^2effective mode areas respectively. For the three conventional structures of similar parameters the values of nonlinear coefficient are found close to each other (3.43$W^{-1}km^{-1}$, 2.865$W^{-1}km^{-1}$ and 2.493 $W^{-1}km^{-1}$ respectively at 1.55 μm) but the Hy-PCF has shown 19.03$W^{-1}km^{-1}$. Moreover the conventional PCFs have provided negligible birefringence of the order of 10^{-6} only, but the Hy-PCF has provided large birefringence (4.34×10^{-3} at 1.55 μm wavelengths).

Considering the overall system performance, it can be said that, this findings of this thesis on PCF structures will help to fabricate better kind of optical transmission media of more data rates. Loss parameter analysis of all structures studied will suggest their application in specific areas of optical communication.

TABLE OF CONTENTS

LIST OF FIGURES

LIST OF TABLES

Number and Title of Tables **Page No**

LIST OF SYMBOLS

A_{eff}	effective mode area
a_R	intrinsic loss
B	magnetic field vector
$D(\lambda)$	chromatic dispersion
D	electric dispersion vector
d	air hole diameter
E	electric field distribution
E	electric field vector
H	magnetic flux density
$I_m[\eta_{eff}]$	imaginary part of effective mode index
J	current density
J_{free}	free current
k	wave vector
K	propagation constant
k_o	free space wave number
L	fiber length
L_c	confinement loss
T_g	group delay
α	delay rate
$\alpha(\lambda)$	loss spectrum
β	wave propagation constant
β_m	modal birefringence
Λ	pitch
Φ	critical angle
Ω	angular frequency

LIST OF ABBREVIATION

SMF	Single-Mode Fiber
LED	Light Emitting Diode
EMI	Electromagnetic Interference
RFI	Radio Frequency Interference
EMPs	Electromagnetic Pulses
TIR	Total Internal Reflection
PBG	Photonic Band Gap
RDS	Relative Dispersion Slope
FEM	Finite Element Method
FDTD	Finite Difference Time Domain
DF-PCF	Dispersion Flattened PCF
ESM	Endlessly Single Mode
ISI	Inter Symbol Interference
PMD	Polarized-Mode Dispersion
PML	Perfectly Matched Layer

CHAPTER 1

INTRODUCTION

1.1 Introduction

Telecommunication is the technology of transferring or receiving signals and messages over long distances using electronic equipment. This is a broad term that includes a wide range of information transmitting technologies such as telephones (wired and wireless), microwave communications, fiber optics, satellites, radio and television broadcasting. Sophisticated techniques have been developed for the modification of the telecommunication system to meet up with the demand of ever increasing consumer all around the world. Among the most frequently used telecommunication system, the fiber optic based communication system is notable. Optical fiber is used by many telecommunication companies to transmit telephone signals, internet communication and cable television signals. The use of the fiber-optic based technology is increasing day by day.

Fiber optic communication is a method of transmitting information from one place to another by sending pulses of light through an optical fiber. The light forms an electromagnetic carrier wave that is modulated to carry information. Fiber is preferred over other means of communication media when high bandwidth, long distance or immunity to electromagnetic interference is required. Fiber optic data transmission systems send information over fiber by converting electrical signals into light. The electromagnetic spectrum is composed of visible and near infrared light like that transmitted fiber.

An optical fiber is a flexible, transparent fiber made by drawing glass (silica) or plastic to a diameter slightly thicker than that of a human hair. Optical fibers are used most often as a means to transmit light between the two ends of the fiber and find wide usage in fiber optic-communication, where they permit transmission over longer distance and at higher bandwidths (data rates) than wire cables.

Fiber optic technology has developed tremendously over last few years and today it is found in many places such as in telecommunication system, military application, medical equipment etc. Fibers are used instead of metal wires because signals travel along them with negligible loss. Fibers are also used for illumination and imaging and are often wrapped in bundles so that they may be used to carry light into, or images out of confined spaces, as in a case of electro-medical equipment.

1.2 Basic Communication System

Communication system is a collection of individual communications, networks, transmission systems, relay stations, and data terminal equipment. A block schematic of a general communication system is shown in Fig. 1.1. The function of which is to convey the signal from the information source over the transmission medium to the destination.

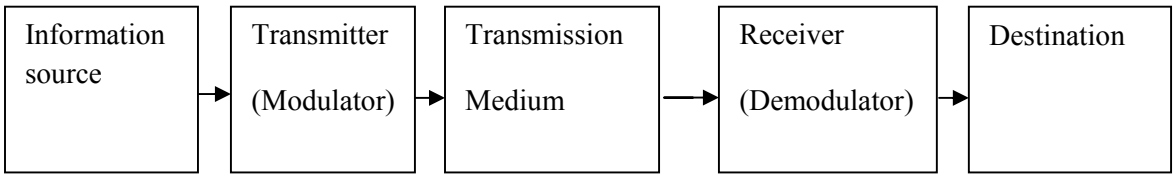

Fig. 1.1**:** The general communication system [1].

The communication system therefore consists of a transmitter or modulator linked to the information source, the transmission medium, and a receiver or demodulator at the destination point. In electrical communications the information source provides an electrical signal, usually derived from a message signal which is not electrical (e.g. sound). The transmitter comprising of electrical and electronic components converts the signal into a suitable form for propagation over the transmission medium. This is often achieved by modulating a carrier, which, as mentioned previously, may be an electromagnetic wave. The transmission medium can consist of a pair of wires, a coaxial cable or a radio link through free space down which the signal is transmitted to the receiver, where it is transformed into the original electrical information signal (demodulated) before being passed to the destination. In any transmission medium the signal is attenuated, or suffers loss, and is subject to degradations due to contamination by random signals and noise, as well as possible distortions imposed by mechanisms within the medium itself. In any

communication system there is a maximum permitted distance between the transmitter and the receiver beyond which the system effectively ceases to give intelligible communication. For long haul applications these factors necessitate the installation of repeaters or line amplifiers at intervals, both to remove signal distortion and to increase signal level before transmission is continued down the link.

1.3 Optical Fiber Communication System

1.3.1 Structure of Optical Fiber

The optical fiber considered in the preceding sections with a core of constant refractive index n_1, cladding of a slightly lower refractive index n_2 is known as step index fiber. This is because the refractive index profile for this type of fiber makes a step change at the core-cladding interface. The refractive index profile may be defined as:

$$n(r) = n_1, \qquad r < a \text{ (core)} \tag{1.1}$$

$$= n_2, \qquad r \geq a \text{ (cladding)} \tag{1.2}$$

However, for lower bandwidth applications multimode fibers have several advantages over single-mode fibers. These are:

(a) The use of spatially incoherent optical sources (e.g. most light-emitting diodes) which cannot be efficiently coupled to single-mode fibers, (b) larger numerical apertures, as well as core diameters, facilitating easier coupling to optical sources, (c) lower tolerance requirements on fiber connectors.

Multimode step index fibers allow the propagation of a finite number of guided modes along the channel. The number of guided modes is dependent upon the physical parameters (i.e. relative refractive index difference, core radius) of the fiber and the wavelengths of the transmitted light. Graded index fibers do not have a constant refractive index in the core but a decreasing code index n_2 with radial distance from a maximum value of n_1 at the axis to a constant value n_2 beyond the core radius a in the cladding. This index variation may be represented as:

$$n(r) = n_1(1-2\Delta(r/a)^{\alpha})^{1/2} \qquad r < a \text{ (core)} \qquad (1.3)$$

$$n_1(1-2\Delta)^{1/2} = n_2 \qquad r \geq a \text{ (cladding)} \qquad (1.4)$$

Using the concepts of geometric optics, the gradual decrease in refractive index from the center of the core creates much refractive of the rays as they are effectively incident on a large number of high to low index interfaces. With an ever increasing angle of incidence, until the conditions for total internal reflection are met, and the ray travels back towards the core axis, again being continuously refracted.

1.3.1.1 Basic Structure

An optical fiber is a thin cylinder of dielectric material able to transport light. The beam launched into the fiber is propagated by total internal reflection. A simple thin cylinder of glass acts as an optical fiber, however it is extreme fragile and breaks easily by applying a small bend. A way to reduce this fragility is to coat the rod with a smooth material like acrylic, silicon or polyimide. The fiber is now much more robust and flexible. However, the light cannot anymore transmit inside the fiber since these protective layers have similar or higher refraction index than the rod and therefore no more internal reflection occurs! To solve this problem, the rod (it will become the core of the fiber) is surrounded by a layer of glass (called cladding) with a small refraction index to permit total internal reflection. The refraction index difference between the core and the clad defines the angle (numerical aperture) at which the light can enter into the fiber. The core diameter ranges from few microns up to few millimeters. The length may reach kilometers as in the case of telecommunications applications. Optical fibers may be classified according to the following ways:

(i) Single-mode Fiber

In fiber-optic communication, a single-mode optical fiber (SMF) is an optical fiber designed to carry light only directly down the fiber - the transverse mode. Modes are the possible solutions of the Helmholtz equation for waves, which is obtained by combining Maxwell's equations and the boundary conditions. These modes define the way the wave travels through space, i.e. how the wave is distributed in space. Waves can have the same

mode but have different frequencies. This is the case in single-mode fibers, where we can have waves with different frequencies, but of the same mode, which means that they are distributed in space in the same way, and that gives us a single ray of light. Although the ray travels parallel to the length of the fiber, it is often called transverse mode since its electromagnetic oscillations occur perpendicular (transverse) to the length of the fiber.

(ii) Multimode Fiber

In a multimode fiber, the core diameter is much bigger than the wavelength of the transmitted light. A number of modes can be simultaneously transmitted. Fiber modes are related to the possible ways the light travels inside the fiber. The primary mode travels parallel to the axis of the fiber and therefore takes the minimum time to reach the end of the fiber. When the incoming beam enters with an angle respect to the fiber axis, the light will follow a longer path and therefore will take longer to reach the end. The number of modes that can be transmitted along the fiber increases with the core diameter. Multimode fibers may be divided in step and graded index.

(iii) Step-Index Fiber

Step index fibers are the most used fibers in fields other than telecommunications. The refraction index of the core is constant in these and the light travels in straight paths. They are relatively cheap and they have the widest range of core diameters: basically from 50 μm up to 2mm. The material may be plastic, liquid or glass. Plastic fibers are not wide used nowadays; their optical transmission is poor and the core relatively big (0.5 to 2 mm). The most efficient fibers are made in acrylic and they are mainly used for short length telecommunication networks. In spite of their limited performances, new developments in plastic fibers might open applications in the field of high speed home networks (Gigabit/s). New polymers are being proposed with attenuations approaching the silica fibers.

(iv) Graded-Index Fiber

In fiber optics graded index is an optical fiber whose core has a refractive index that decreases with increasing radial distance from the optical axis of the fiber. Because parts of the core closer to the fiber axis have a higher refractive index than the parts near the

cladding, light rays follow sinusoidal paths down the fiber. The most common refractive index profile for a graded-index fiber is very nearly parabolic. The parabolic profile results in continual refocusing of the rays in the core, and minimizes modal dispersion.

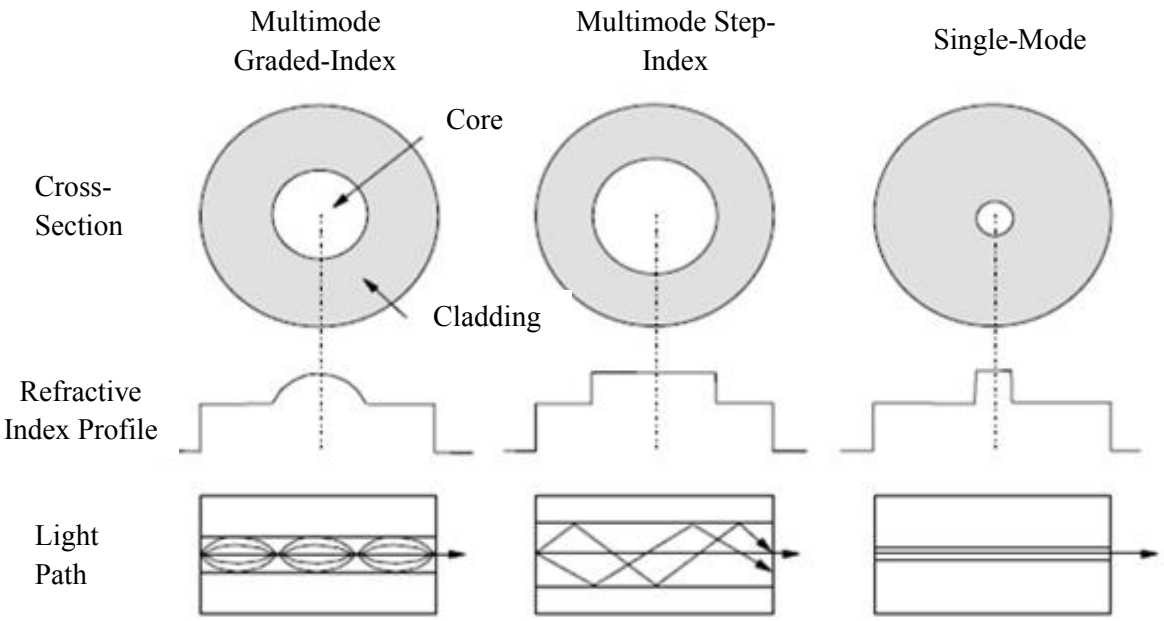

Fig. 1.2**:** The different types of optical fiber.

(v) Multi-core Fiber

Multi-Core Fiber (MCF) is a revolutionary new approach to engineer a fiber for high capacity applications. MCF prototypes in both single-mode (SM) and multi-mode (MM) with a multiple of cores ranging from 4 to 8 have been produced. Application of MCF includes in metro optical networks, wireless base stations, data center connectivity, next-generation optical amplifiers, down-hole sensing in oil exploration applications, pipeline monitoring, backplane and inter-chip communications.

1.3.1.2 Concept of Basic Optical Fiber Communication

An optical fiber communication system is similar in basic concept to any type of communication system. The simplest type of fiber-optic communication system is a fiber-optic link providing a point to point connection with a single data channel. For optical fiber communications the system is shown in Fig 1.3.

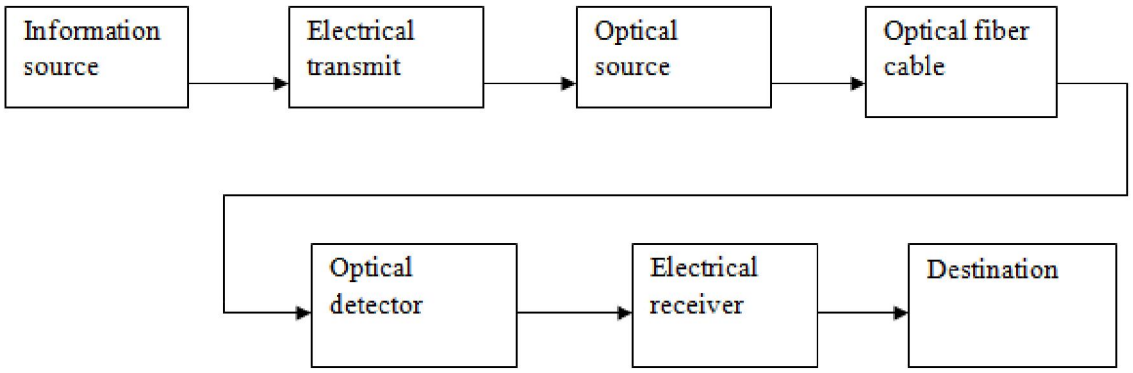

Fig 1.3: The optical fiber communication system [1].

In this case the information source provides an electrical signal to a transmitter comprising an electrical stage which drives an optical source to give modulation of the light wave carrier. The optical source which provides the electrical–optical conversion may be either a semiconductor laser or light-emitting diode (LED). The transmission medium consists of an optical fiber cable and the receiver consists of an optical detector which drives a further electrical stage and hence provides demodulation of the optical carrier. Photodiodes and, in some instances, phototransistors and photoconductors are utilized for the detection of the optical signal and the optical–electrical conversion. There is a requirement for electrical interfacing at either end of the optical link and at present the signal processing is usually performed electrically. The optical carrier may be modulated using either an analog or digital information signal. In the system shown in Fig 1.2 analog modulation involves the variation of the light emitted from the optical source in a continuous manner. With digital modulation, however, discrete changes in the light intensity are obtained (i.e. on–off pulses). Although often simpler to implement, analog modulation with an optical fiber communication system is less efficient, requiring a far higher signal-to-noise ratio at the receiver than digital modulation. The linearity needed for analog modulation is not always provided by semiconductor optical sources, specially at high modulation frequencies. For these reasons, analog optical fiber communication links are generally limited to shorter distances and lower bandwidth operation than digital links.

1.3.2 Ray Optics Theory

The refractive index of a medium is defined as the ratio of the velocity of light in a vacuum to the velocity of light in the medium. A ray of light travels more slowly in an optically dense medium than in one that is less dense, and the refractive index gives a measure of this effect.

When a ray is incident on the interface between two dielectrics of differing refractive indices (e.g. glass–air), refraction occurs, as illustrated in Fig 1.4. It may be observed that the ray approaching the interface is propagating in a dielectric of refractive index n_1 and is at an angle Φ_1 to the normal at the surface of the interface. If the dielectric on the other side of the interface has a refractive index n_2 which is less than n_1, then the refraction is such that the ray path in this lower index medium is at an angle Φ_2 to the normal, where Φ_2 is greater than Φ_1. The angles of incidence Φ_1 and refraction Φ_2 are related to each other and to the refractive indices of the dielectrics by Snell's law of refraction [1], which states that:

$$n_1 \sin\Phi_1 = n_2 \sin\Phi_2 \qquad (1.5)$$

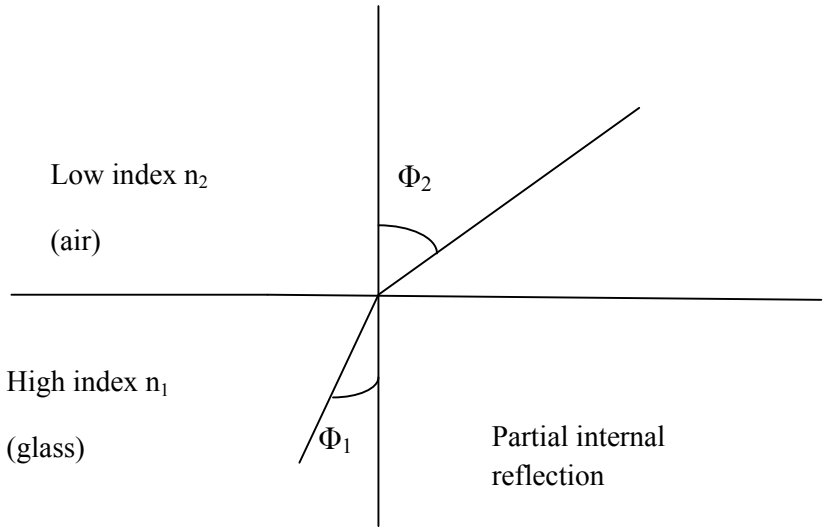

Fig. 1.4**:** Incident light rays and refracted light rays [1]

It may also be observed in Fig. 1.3 that a small amount of light is reflected back into the originating dielectric medium (partial internal reflection). As n_1 is greater than n_2, the angle of refraction is always greater than the angle of incidence. Thus when the angle of

refraction is 90° and the refracted ray emerges parallel to the interface between the dielectrics, the angle of incidence must be less than 90°. This is the limiting case of refraction and the angle of incidence is now known as the critical angle Φ_c, as shown in Fig. 1.5.

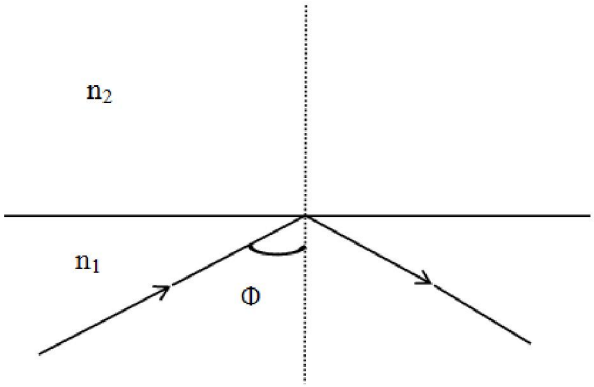

Fig. 1.5: The limited case of refraction and critical ray [1].

The value of the critical angle is given by:

$$\sin\Phi_c = n_2/n_1 \tag{1.6}$$

At angles of incidence greater than the critical angle the light is reflected back into the originating dielectric medium (total internal reflection) with high efficiency (around 99.9%). It may be observed in Fig. 1.6.

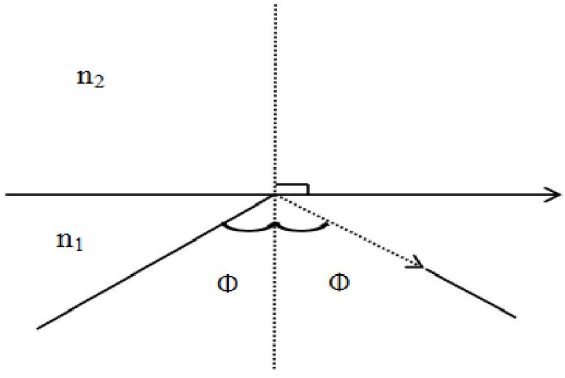

Fig. 1.6: Total internal reflection [1].

1.3.3 Geometry of Optical Fiber

In its simplest form an optical fiber consists of a cylindrical core of silica glass surrounded a cladding whose refractive index is lower than that of the core. Because of an abrupt index change at the core–cladding interface, such fibers are called step-index-fiber. In a different type of fiber, known as graded-index-fiber, the refractive index decreases gradually inside the core. Fig. 1.7 shows schematically the index profile and the cross section for the two kinds of fibers.

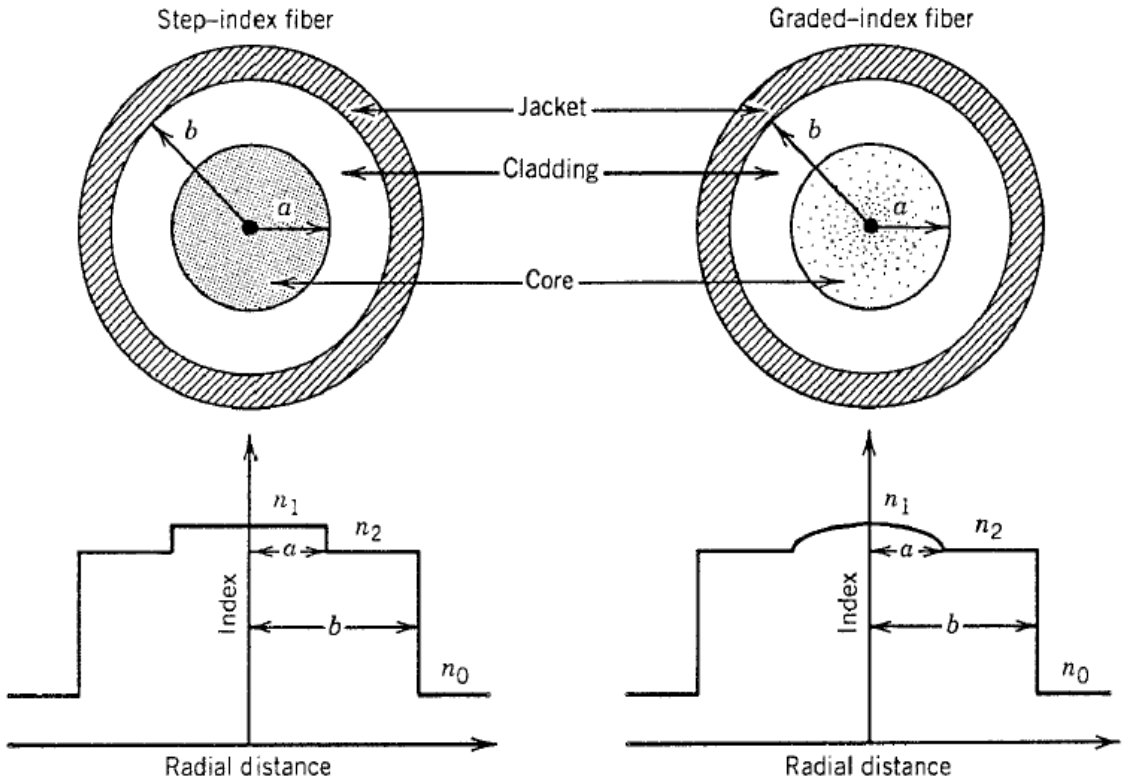

Fig. 1.7: Cross-section and refractive-index profile of step-index and graded-index fiber [2]

A step-index profile is a refractive index profile characterized by a uniform refractive index within the core and a sharp decrease in refractive index at the core-cladding interface so that the cladding is of a lower refractive index. Fig. 1.8 shows the light confinement through total internal reflection in step index fibers.

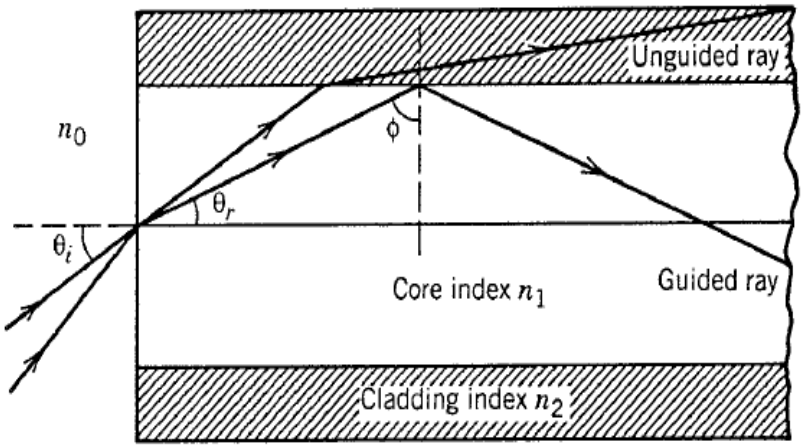

Fig. 1.8: Light propagation in step-index fiber [2].

The refractive index of the core in graded-index fibers is not constant but decreases gradually from its maximum value n_1 at the core center to its minimum value n_2 at core–cladding interface. Most graded-index fibers are designed to have a nearly decrease and are analyzed by using following equations

$$n(\rho) = \begin{cases} n_1[1 - \Delta(\rho/a)^{\alpha}]; & \rho < a, \\ n_1(1 - \Delta) = n_2 \ ; & \rho \geq a, \end{cases}$$

where a is the core radius. Light propagation in graded-index fiber is shown in Fig. 1.9.

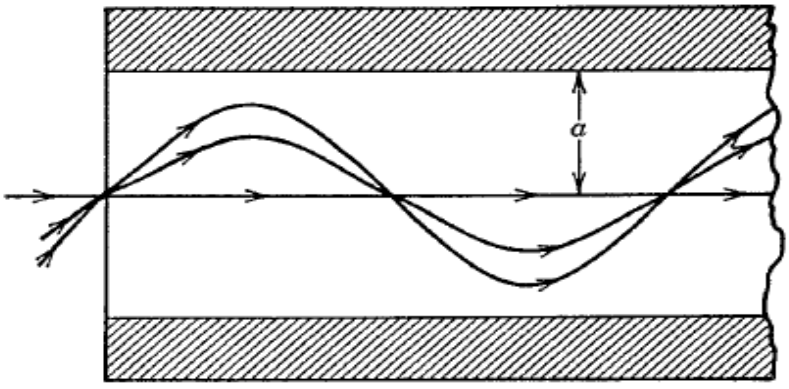

Fig. 1.9: Light propagation in graded-index fiber [2].

1.3.4 Benefits of Optical Fiber Communication System

It is useful to consider the merits and special features offered by optical fiber communications over more conventional electrical communications. In this context we will discuss about the benefits of optical fiber communication system

(i) Enormous Bandwidth: The optical carrier frequency in the range 10^{13} to 10^{16} Hz yields a far greater potential transmission bandwidth than metallic cable systems (i.e. coaxial cable bandwidth typically around 20 MHz over distances up to a maximum of 10 km) or even millimeter wave radio systems (i.e. systems currently operating with modulation bandwidths of 700 MHz over a few hundreds of meters).

(ii) Small Size and Weight: Optical fibers have very small diameters which are often no greater than the diameter of a human hair. Hence, even when such fibers are covered with protective coatings they are far smaller and much lighter than corresponding copper cables.

(iii) Electrical Isolation: Optical fibers which are fabricated from glass, or sometimes a plastic polymer, are electrical insulators and therefore, unlike their metallic counterparts, they do not exhibit earth loop and interface problems. Furthermore, this property makes optical fiber transmission ideally suited for communication in electrically hazardous environments as the fibers create no arcing or spark hazard at abrasions or short circuits.

(iv) Immunity to Interference and Crosstalk: Optical fibers form a dielectric waveguide and are therefore free from electromagnetic interference (EMI), radio-frequency interference (RFI), or switching transients giving electromagnetic pulses (EMPs). Hence the operation of an optical fiber communication system is unaffected by transmission through an electrically noisy environment and the fiber cable requires no shielding from EMI. The fiber cable is also not susceptible to lightning strikes if used overhead rather than underground. Moreover, it is fairly easy to ensure that there is no optical interference between fibers and hence, unlike communication using electrical conductors, crosstalk is negligible, even when many fibers are cabled together.

(v) Signal Security: The light from optical fibers does not radiate significantly and therefore they provide a high degree of signal security. Unlike the situation with copper

cables, a transmitted optical signal cannot be obtained from a fiber in a noninvasive manner (i.e. without drawing optical power from the fiber). Therefore, in theory, any attempt to acquire a message signal transmitted optically may be detected. This feature is obviously attractive for military, banking and general data transmission (i.e. computer network) applications.

1.3.5 Optical Transmission Windows

One of the principle characteristics of an optical fiber is its attenuation as a function of wavelength, as shown in Fig. 1.10 .Early applications in the late 1970s made exclusive use of the 770 to 910 nm wavelength band. This wavelength region was referred as the first window. The centre of the first window was around 850 nm. The second window was centered at 1310 nm and the third window was centered at 1550 nm. In the Fig., the dashed vertical lines indicate the centers of the three traditional operating wavelength bands of optical fiber systems, which are short wavelength region, the O-band and C-band.

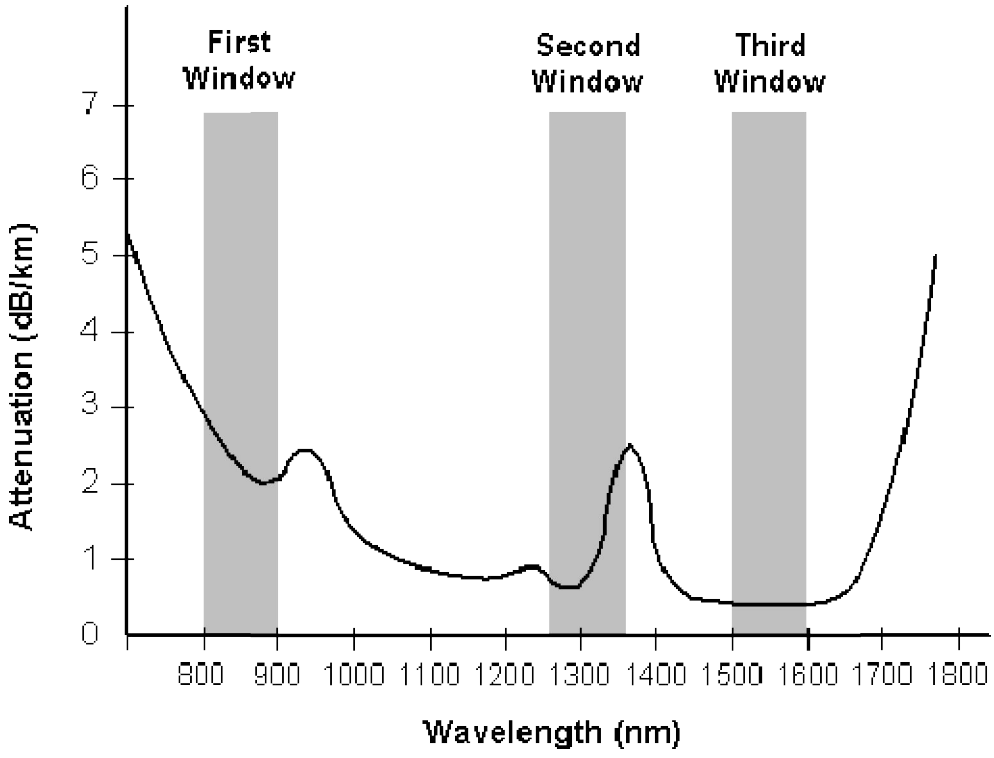

Fig. 1.10: Transmission windows of optical fiber [3].

1.4 Photonic Crystal Fiber (PCF)

1.4.1 Basic Concept of PCF

A new optical fiber structure was demonstrated in early 1990s which was known as Photonic Crystal Fiber (PCF). The difference between this new structure and that of a conventional fiber is that the cladding and in some cases, the core regions of a PCF contains air holes, which run along the entire length of the fiber whereas the material properties of the core and cladding define the light transmission characteristic of conventional fibers. The structural arrangement in a PCF creates an internal microstructure, which offers extra dimensions in controlling the optical properties of light, such as the dispersion nonlinearity and birefringence effects in optical fiber. Two types of PCFs come in two basic varieties. One is solid core and another one is hollow core.

1.4.1.1 Solid Core PCF

Like conventional fibers, solid-core PCF's guide light by Total Internal Reflection (TIR) at the boundary between a low index cladding and a high index core. In most all-solid fibers the required index difference is created by doping either the core or the cladding glass. In a PCF the same is achieved by incorporating holes into the cladding, causing the weighted average refractive index "seen" by the mode to be lower than that of the core. By altering the arrangement of holes or the shape of the core, optical properties such as mode shape, non-linearity, dispersion, and birefringence can be varied over a range, often well exceeding what is possible with conventional fiber technology. As the distribution of light between air and glass changes with wavelength, so does the average index. This can be exploited to create fibers with very large amounts of dispersion of both signs or, indeed, of very low dispersion by using the wavelength dependence of the effective index to compensate for material and waveguide dispersion. Similarly, it is easy to incorporate more than one core into the photonic crystal cladding, allowing one to form arrays of coupled or independent waveguide. In solid core PCFs, as in all TIR fibers, the vast majority of light propagates in the glass. Construction of a solid core PCF is given in Fig. 1.11.

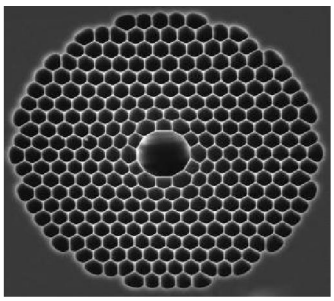

Fig. 1.11: Solid core PCF

1.4.1.2 Hollow Core Fibers

Hollow core fibers guide light in a hollow core that is surrounded by a micro-structured cladding. Photonic band gaps can form in materials that have a periodically structured refractive index; in PCFs this is achieved by using a periodic arrangement of air holes in silica. These fibers are sold based on the overall optical specifications and not the physical structure. A construction of hollow core fiber is shown in Fig. 1.12.

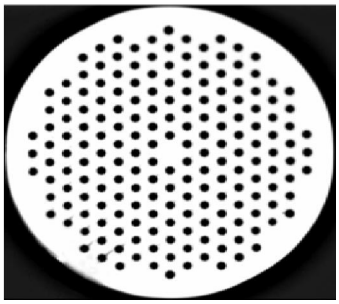

Fig. 1.12: Hollow core fiber

1.4.2 History of PCF

The original motivation for developing PCFs was the creation of a new kind of dielectric waveguide that guides light by means of a two-dimensional (2-D) PBG. In 1991, the idea that the well-known "stop bands" in periodic structures could be extended to prevent propagation in all directions was leading to attempts worldwide to fabricate three-dimensional PBG materials. At that time, the received wisdom was that the refractive-index difference needed to create a PBG in two dimensions was large of order 2.2:1. It was not widely recognized that the refractive-index difference requirements for PBG formation in

two dimensions are greatly relaxed if, as in a fiber, propagation is predominantly along the third axis.

PCFs were made to trap light in a hollow core by means of a 2-D “photonic crystal” of microscopic air capillaries running along the entire length of a glass fiber. Appropriately designed, this array would support a PBG for incidence from air, preventing the escape of light from a hollow core into the photonic-crystal cladding and avoiding the need for TIR.A question sometimes asked is whether these developments were really “new” or whether some aspects could be traced to previous work. While it is clear that no previous attempt had been made to produce photonic-crystal lattices of air holes in fiber form, or to create PBGs, there had been previous work on microstructure fibers. For example, in the 1970s, “single-component” fibers were investigated in which a central glass strand was held in place by two thin webs of glass. In the 1980s, fiber polarizer’s were developed at Southampton by drawing fibers with hollow side-channels (~30μm in diameter) for introducing metal wires. In 1993, with funding from the Defence Research Agency in Malvern, U.K., work began in earnest, the initial idea being to adapt techniques widely used for the fabrication of multichannel image intensifier plates. These are made by stacking individual cylindrical elements into a 2-D close-packed array, the end result after drawing being a honeycomb of ~ 10 μ m diameter waveguide “pixels,” each surrounded by black glass to reduce crosstalk. They also considered adapting techniques developed at the Naval Research Laboratory, Washington, DC, where cores from soluble glass, surrounded by insoluble glass, are arranged in a close-packed lattice and drawn down to microscopic dimensions. The soluble glass can then be dissolved out, leaving an array of tiny hollow channels in plates as thick as 200μm.At this time, the parallel task of solving Maxwell’s equations numerically was making good progress, culminating in a 1995 paper that showed that PBGs did indeed exist in 2-D silica–air structures for “conical” incidence from vacuum—this being an essential prerequisite for hollow-core guidance. The first successful silica–air PCF structure was made in late 1995 by stacking 217 silica capillaries (eight layers outside the central capillary), specially machined with hexagonal outer cross sections and a circular inner cross section. The diameter-to-pitch ratio d/Λ of the holes in the final stack was ~ 0.2,which theory showed was too small for PBG guidance in a hollow core, so we decided to make a PCF with a solid central core surrounded by 216 air channels. This

led to the discovery of ESM PCF, which, if it guides at all, only supports the fundamental guided mode. The success of these initial experiments led rapidly to a whole series of new types of PCF—large mode area, dispersion controlled hollow-core, birefringent, and multi-core. These initial breakthroughs led quickly to applications, perhaps the most celebrated being the report in 2000 of SC generation from unamplified second laser pulses in a PCF with a core small enough to give zero dispersion at 800 nm wavelength.

1.4.3 Types of PCF

Photonic crystal fiber can be classified as mainly two types. Index-guided PCF and Photonic Band gap PCF.

1.4.3.1 Index Guided PCF

Although the principles of guidance and the characteristics of index-guided PCFs are similar to those of conventional fiber, there is greater index contrast since the cladding contains air holes with a refractive index of 1 in comparison with the normal silica cladding index of 1.457 which is close to the germanium-doped core index of 1.462. A fundamental physical difference, however, between index-guided PCFs and conventional fibers arises from the manner in which the guided mode interacts with the cladding region. Whereas in a conventional fiber this interaction is largely first order and independent of wavelength, the large index contrast combined with the small structure dimensions cause the effective cladding index to be a strong function of wavelength. For short wavelengths the effective cladding index is only slightly lower than the core index and hence they remain tightly confined to the core. At longer wavelengths, however, the mode samples more of the cladding and the effective index contrast is larger. This wavelength dependence results in a large number of unusual optical properties which can be tailored. For example, the high index contrast enables the PCF core to be reduced from around 8μm in conventional fiber to less than 1 μm, which increases the intensity of the light in the core and enhances the nonlinear effects. Two common index-guided PCF designs are shown diagrammatically in Fig. 1.13.

Fig. 1.13: Two index-guided photonic crystal fiber structures [1].

1.4.3.2 Photonic Band Gap fibers

Photonic band gap (PBG) fibers are a class of micro structured fiber in which a periodic arrangement of air holes is required to ensure guidance. This periodic arrangement of cladding air holes provides for the formation of a photonic band gap in the transverse plane of the fiber. As a PBG fiber exhibits a two-dimensional band gap, then wavelengths within this band gap cannot propagate perpendicular to the fiber axis (i.e. in the cladding) and they can therefore be confined to propagate within a region in which the refractive index is lower than the surrounding material. Hence utilizing the photonic band gap effect light can, for example, be guided within a low-index, air-filled core region creating fiber properties quite different from those obtained without the band gap. Although, as with index-guided PCFs, PBG fibers can also guide light in regions with higher refractive index, it is the lower index region guidance feature which is of particular interest. In addition, a further distinctive feature is that while index-guiding fibers usually have a guided mode at all wavelengths, PBG fibers only guide in certain wavelength bands, and furthermore it is possible to have wavelengths at which higher order modes are guided while the fundamental mode is not. Two important PBG fiber structures are displayed in Fig. 1.14.

Fig. 1.14: Photonic band gap (PBG) fiber (a) Honeycomb PBG (b) air-guiding PBG [1]

1.4.4 Application of PCF

PCFs have been used to realize various optical components and devices including long period gratings, multimode interference power splitters, tunable coupled cavity fiber lasers, fiber amplifiers, multichannel add/drop filters, wavelength converters and wavelength de-multiplexers. As with conventional optical fibers, however, a crucial issue with PCFs has been the reduction in overall transmission losses which were initially several hundred decibels per kilometer even with the most straightforward designs. Since light can be guided in PCFs by embedding a region of solid glass within an array of air holes, this approach has several important applications, and an excellent introduction is available in a recent review. Index-guiding PCFs offer a wealth of new opportunities, both to those interested in fundamental fiber optics and to those looking to extend its applications. These opportunities stem from just a few special properties of the photonic crystal cladding, which are caused by the large refractive index contrast and the 2D nature of the microstructure. These affect the dispersion, the smallest attainable core size, and the number of guided modes, the numerical aperture and the birefringence. For example, group velocity dispersion can be radically affected by pure waveguide dispersion in fibers with small cores and large air holes in the cladding. It can also be more subtly engineered, using the dispersion of the photonic crystal material itself, so as to cancel the combined effects of the bulk silica dispersion and the waveguide dispersion over a broad wavelength range. Such dispersion engineering enables the generation of a single- mode broadband optical super continuum, which is a spectacular light source that is already being used for frequency metrology and optical coherence tomography 22. Other properties of the fibers can be engineered: one can create structures with enormous birefringence or that support only a single mode that is independent of the wavelength. Such structures are leading to novel sensors high-power fiber lasers and to developments in other research fields

1.5 An Overview of Previous Researches on PCF

Researchers and engineers in several laboratories around the world are working on ways to revolutionize fiber-optic design and performance. To be competitive with existing telecommunication technology, new fibers would have to perform at least as well as conventional fibers overall and deliver significantly improved performance in some

respects. In the recent years, PCFs have attracted much interest among the researchers as they rely on the unusual properties of photonic crystals to deliver previously unimaginable performance from an optical fiber waveguide. Thus superiority of PCFs in several respects are being demonstrated, which is leading to new applications. Some of their works are reviewed below:

In paper [4] **"A new circular photonic crystal fiber for effective dispersion compensation over E to L wavelength bands"**, M. M. Haque, M. S. Rahman, M. Samiul Habib, M. Selim Habib and S. M. A. Razzak presented a new circular photonic crystal fiber (C-PCF) for effective dispersion compensation covering E to L wavelength bands ranging from 1360-1625 nm. The use of only five air-hole rings and silica as the material has made the structure quite simple for fabrication process. From their numerical simulation, it is found that the designed C-PCF simultaneously shows a large negative dispersion of about −248.65 to −1069 ps/(nm.km) and a relative dispersion slope (RDS) exactly equal to that of a single mode fiber (SMF) at 1.55 μm wavelength. The residual dispersion after compensating 40 km long SMF is within ±62 ps/nm-km which ensured its application in high speed WDM system. Besides, dispersion slope, slope compensation ratio, effective area and confinement loss of the proposed C-PCF are also evaluated and discussed in the paper.

In paper [5] **"Chromatic dispersion control in photonic crystal fibers: application to ultra-flattened dispersion"**, K. Saitoh and M. Koshiba reported a new controlling technique of chromatic dispersion in PCF in order to control the dispersion and the dispersion slope of index-guiding PCFs. Using this technique they have shown designed PCF with both ultra-low dispersion and ultra-flattened dispersion in a wide wavelength range. It is shown from numerical results that it is possible to design a four ring PCF with flattened dispersion of 0 ± 0.5 ps/ km-nm from a wavelength of 1.19 μm to 1.69 μm and a five-ring PCF with flattened dispersion of 0 ± 0.4 ps/km-nm from a wavelength 1.23 μm to 1.72 μm setting the hole-to-hole spacing as 2.6 μm and the air-hole diameter 0.0624 μm respectively

In paper [6] **"Dispersion analysis of a Hybrid Photonic Crystal Fiber"** Dinesh Kumar Prajapati and Ramesh Bharti proposed a new PCF structure which is suitable for optical

telecommunications. They also compared and analyzed the design of Hybrid PCF with circular air hole and elliptical air holes for the total dispersion property of both the configuration. By varying the size of the air holes they have obtained flattened dispersion for the wavelength range 1.1 μm to 1.5 μm range. For the entire configurations analyzed the mean cladding refractive index was lower than the core index. It is observed that all the structures proposed in this paper have shown the most negative (zero order) dispersion in between the wavelength range of 1.0 μm to 1.5 μm. But HPCF structure with Elliptical Air holes having the more flattened dispersion characteristics compare than other two structures (circular air holes).

In paper [7] **"Numerical investigation and optimization of a photonic crystal fiber for simultaneous dispersion compensation over *S* + *C* + *L* wavelength bands"** by K. Varshney, N. J. Florous, K. Saitoh, M. Koshiba, and T. Fujisawa, an optimized PCF design was proposed which can eliminate the residual dispersion from the transmission link after dispersion compensation and can also provide a simultaneous dispersion compensation for the signal channels from S to L band. A dispersion of −98.3 ps/km-nm can be realized with a variance of +/−0.55 ps/km-nm from 1480 nm to 1630 nm with a dispersion slope of 0.005 ps/nm-km at 1550 nm. Here, the design comprises of 11 air-hole rings with silica as a background material. The air holes diameter for the 1st ring d1= 0.637μm,for 2nd ring d2=0.215 μm and for 3rd to 11th ring d3=0.592 μm and pitch, Λ=1.05 μm were taken for the optimized design. It was found thata +/− 2% change in the fiber parameters may lead to a +/− 8% shift of the dispersion from its nominal value.

A paper titled [8], **"Large negative dispersion ultra flattened hybrid photonic crystal fiber for residual dispersion compensation over 750 nm bandwidth"**, by Shobug at el, a hybrid photonic crystal fiber consisting of hexagonal and octagonal rings is presented for the compensation of residual dispersion in the range of 1260-2000 nm. Hexagonal structure is used to control the dispersion characteristics and octagonal structure is used to control the confinement loss characteristics.The designed PCF shows ultra-flattened average negative dispersion of –110.21ps/nm-km with an absolute dispersion variation of 1.49 ps/nm-km. The geometry of the design has 7 air hole rings with all the air hole rings are taken circular. The effective area of the fiber at 1550 nm is 4.2 μm^2. The confinement loss is found to be

high and this value is 0.01dB/m at 1550 nm. Confinement loss in Hy PCF is much lower than normal hexagonal structured PCF due to more air-holes in the cladding region for same ring.

In paper [9] **"Design of Highly Birefringent and Low Confinement Loss Photonic Crystal Fiber by Introducing Asymmetric Defect Structures"** the authors Lukman V and Jeena Maria Cherian proposed two highly birefringent PCF with ultra-low confinement loss by introducing four ring solid core hexagonal structure which having both elliptical and circular air holes and introducing large air hole diameters near the core region for making the asymmetry.). An endlessly single mode, high birefringent (05.152x10-3) and a low confinement loss (7.85x10-5 dB/km) is found at the excitation wavelength of λ=1550 nm with only four rings of air holes in the fiber cladding.

In paper [10] **"Double-cladding rectangular-lattice birefringence photonic crystal fiber with elliptical air holes"** Wan Zhang, Shu-guang Li, Guo-Wen An, Zhen-Kai Fan and Ya-Jie Bao proposed a novel design of PCF with the characteristics of high birefringence and zero dispersion. The structure is composed of the rectangular lattice with double-cladding and there is an elliptical air hole in the core of the PCF having the same size with the holes of inner ring. Their obtained birefringence value is 2.19×10^{-3} at 1.31μm and 2.99×10^{-3} at 1.55 μm wavelengths respectively which suggests that this fiber will play a very important role in the fields of polarization maintaining transmission system and zero dispersion devices.

In paper [11] **"Ultra-flattened dispersion hexagonal photonic crystal fibre with low confinement loss and large effective area"** Saeed Olyaee and Fahimeh Taghipour discussed about a PCF which has some features including low- and ultra-flattened dispersion and low confinement loss as well as a large effective area in a wide range of wavelengths. The dispersion value is less than 2.5 ps/nm-km with small variations of about 0.8 ps/(nm km) in the wavelength range from 1.1 to 1.7 μm. The confinement loss obtained is less than 10^{-6} dB/km in that applicable wavelength range, whereas the effective area is around 61.2 mm^2 at 1.55 μm wavelength. The optimal structural parameters are designed to achieve minimum confinement loss, dispersion and dispersion variation to utilize in broadband optical transmission applications.

In paper [12] **"Theoretical design of a large effective mode area microstructure optical fiber"** S.M.A. Abdur Razzak And Yoshinori Namihira presented a microstructure optical fiber with large effective mode area, low confinement loss, and dispersion-flat property which may be promising for next generation optical data transmission applications. A hexagonal eight ring silica-air microstructure is used with two air-hole dimensions and a common pitch to obtain a very high effective area of the order 122 to 252 μm^2. The design was relatively simpler than the existing designs till that time having large mode area, dispersion-flat response, and low confinement loss in a wide wavelength range.

In paper [13] **"A new design of photonic crystal fiber with ultra-flattened dispersion to simultaneously minimize the dispersion and confinement loss"**, by Saeed Olyaee and Fahimeh Taghipour, a novel design for dispersion flattened PCF (DF-PCF) is proposed. The dispersion slope is 6.8×10^{-4} ps/km.nm^2 and the confinement loss reaches below 10^{-6} dB/km in the wavelength range of 1100 nm to 1800 nm, while at the same time an effective area of more than 50 μm^2 has been attained. This PCF comprises 6 air hole rings, embedded in pure silica with a refractive index of 1.45. This paper shows that lower values of dispersion and confinement loss can be acquired by reducing the diameters of the holes in the inner rings and increasing the size of the holes in the outer rings.

In reference [14**] "Highly Nonlinear and Birefringent Spiral Photonic Crystal Fiber"**,spiral photonic crystal fiber with elliptical air holes was designed for achieving high birefringence, large nonlinearity and negative dispersion. The proposed structure has birefringence of the order 10^{-2}, nonlinearity of 26739.42W^{-1} m^{-1}, and dispersion of −1136.69 at 0.85 μm. Due to high birefringence and negative dispersion, the proposed structure can be used for polarization control and dispersion compensation, respectively. So it can be used for nonlinear applicationslike four-wave mixing, supercontinuum generation,and second harmonic generation.

In another paper [15] of Saeed Olyaee and Fahimeh Taghipour named as **"Design of new square-lattice photonic crystal fibers for optical communication applications"** they proposed two new square-lattice PCFs having identical structures with five air-hole rings of different air-hole diameter. Both the fibers exhibit properties of ultra-flattened nearly zero dispersion with slope of about 7×10^{-3} ps/(nm.km) and low confinement loss in

wavelength range of 1.2 to 1.7 μm which highly favors their application as transmission medium in optical communications.

1.6 Objectives of the Thesis

The objectives of this thesis paper are set as under:

(a) To design different structure of PCF to minimize dispersion and other losses.

(b) To carry out the comparative study of the designed structures of PCF for varying parameters of PCF communication.

(c) To study the loss parameters of designed models and investigate the non-linear coefficient in order to explain nonlinearity of the proposed structures.

(d) To find the sensitivity analysis of the modified structure.

1.7 Organization of the Thesis Book

Chapter 1 deals with the introduction of the thesis. This chapter explains the basic concept of communication system, generalized optical fiber communication system, benefits of optical fiber, and basic idea of Photonic Crystal Fiber (PCF).It also contains introductory discussions on PCF history and summary of previous studies on PCF.

Chapter 2 focuses on the theories regarding PCF. A broad discussion about light guiding mechanism through PCF is presented. The various losses of PCF, most importantly dispersion, confinement loss, effective mode area, nonlinearity and birefringence are discussed here. The related equations to analyze the properties of the parameters are described to attain the objectives.

Chapter 3 addresses the structural description of the PCF models designed and proposed for this thesis. The electric field intensity profiles found from COMSOL Multi-Physics 4.4 Simulation Software and by using Finite Element Method (FEM) are presented to analysis electric field distribution and visualize the light confinement of the PCFs.

Chapter 4 presents the results and discussion on graphical presentation of the numerical results obtained from the study and analysis of the propagation properties of the proposed PCF models. The descriptions of the plots found by varying structural parameter are shown for the tolerance analysis of a specific model.

Chapter 5 draws a conclusion of this work. It provides a complete summary of our thesis and highlights the scopes for future works.

CHAPTER 2

TRANSMISSION PROPERTIES OF PHOTONIC CRYSTAL FIBER

2.1 Introduction

Photonic crystal fiber (PCF) is a new class of micro-structured optical fiber and it has been very popular in the field of fiber optic communication because of its confinement characteristics which is not possible in conventional optical fiber. According to their mechanism for confinement PCFs possess two modes of operation—index guiding and photonic band gap fibers In index guiding PCF's, where light is confined in a higher refractive index region, the light is guided by total internal reflection between the solid core and cladding region. Instead, when the core has a refractive index lower than that of the cladding region, as in hollow-core fibers, it is necessary the presence of the photonic band gap (PBG). The presence of air-holes in the cladding gives rise to strong wavelength dependence of the cladding index, which is primarily responsible for PCFs magnificent characteristics. Unlike conventional optical fibers where the doping is necessary to have wave guidance, the light can be guided into PCFs by the presence of holey cladding without doping the core region. One of the first special characteristics to be reported for the PCF is its potential to be endlessly single-mode (ESM) referring to the absence of higher-order modes regardless of the optical wavelength. A PCF which is ESM can in principle be scaled to an arbitrary dimension to remain single-mode. But since the numerical aperture (NA) decreases with increasing mode size, the scaling of the PCF is in general limited by macrobending loss and micro-deformation loss due to the decreasing mode spacing between the guided mode and leaky cladding-modes.

However the current discussion gives an outline of several transmission characteristics and light guidance mechanisms of PCFs in the field of optical communication.

2.2 Light Transmission in PCF

Propagation of light in a fiber structure is best characterized by remembering that when light with free-space propagation constant k encounters an interface between two materials

with refractive indices $n_1$and n_2, the component of the wave vector parallel to the interface remains unchanged during the interaction. This rule is most widely known (Fig. 2.1a) through the law of reflection (that the angle of incidence is equal to the angle of reflection, so that the quantity nk sinθ is preserved in reflection) and the law of refraction (that $n_1\sin\theta = n_2\sin\theta_2$, so that nk sinθ is preserved in transmission as well). To form a guided mode in the core, one needs to introduce light into the core with a value of β that cannot propagate in the cladding. The largest value of β that can exist in an infinite homogeneous medium with refractive index n is $\beta = nk$, with all smaller values of b allowed. The modal index n_m is derived from β since $n_m = \beta/k$. As with any material, a 2D photonic crystal fiber has a maximum β value that can propagate, at a particular frequency, this corresponds to the 'fundamental' mode of an infinite slab of the material, and this value of β defines the 'effective refractive index' of the material . Consequently a solid-core PCF will guide light through a form of total internal reflection (TIR): nonetheless, in many respects they represent a radical departure from conventional fiber optics. However, far more radical fiber designs result from the fact that the range of modal indices supported by photonic crystals have gaps in them. (Fig. 2.1c).

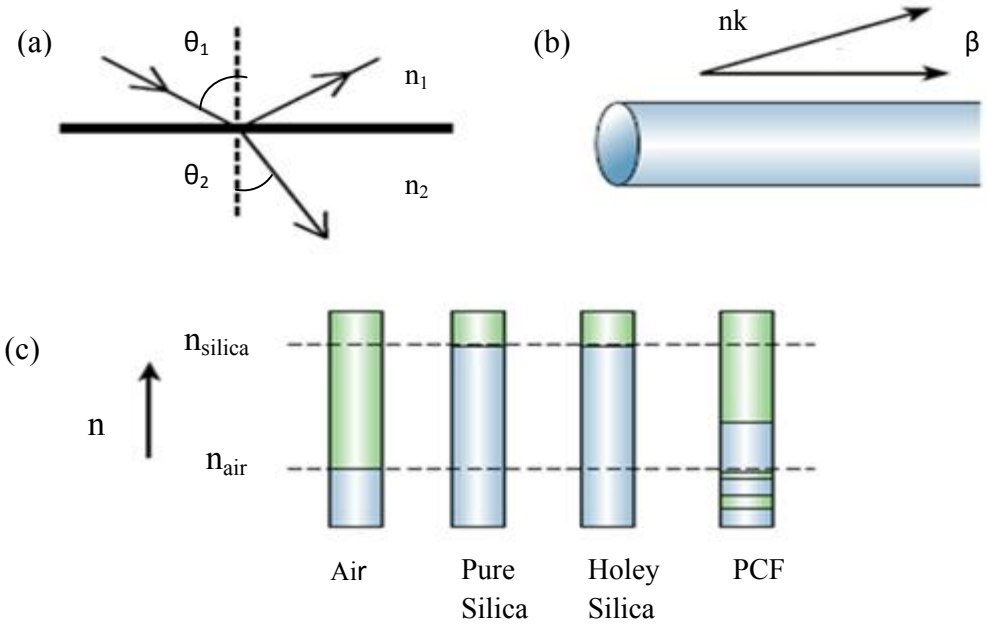

Fig. 2.1: (a) Reflection and refraction (b) Light propagation through fiber optic (c) Allowed values (blue) of modal index.

Fibers with hollow cores cannot be made using conventional optic fibers. This is because guidance by TIR requires a lower-index cladding material surrounding the core, and there are no suitable low-loss materials with a lower refractive index than air at optical frequencies.

2.3 Theory of Electromagnetic Light Propagation through PCF

The basic starting point in understanding the optical properties of photonic crystals is that Maxwell's equations. An electromagnetic wave can be expressed in terms of an electric field vector **E** and a magnetic field vector **B.** When incident on a material the terms **H** the magnetic flux density, **D** the electric displacement vector, J the current density and ρ the charge density are also defined. The Maxwell's equations in the differential form may be expressed in the international system units as:

$$\nabla * \mathbf{E}(\mathbf{r}, \mathrm{t}) = -\mathbf{B}(\mathbf{r}, \mathrm{t}) \tag{2.1a}$$

$$\nabla * \boldsymbol{H}(\boldsymbol{r}, t) = \frac{\partial}{\partial t}\boldsymbol{D}(\boldsymbol{r}, t) + J_{free} \tag{2.1b}$$

$$\nabla * \mathbf{B}(\mathbf{r}, \mathrm{t}) = 0 \tag{2.1c}$$

$$\nabla * \mathbf{D}(\mathbf{r}, \mathrm{t}) = \rho_{\mathrm{free}} \tag{2.1d}$$

Considering a number of assumptions valid for our particular case the previous equations can be simplified. First, for a medium that is free of free charges and free currents, ρ_{free} and J_{free} are set to zero. Next, if the field strengths are assumed to be small enough, the relations $\vec{D}$ to $\vec{E}$ and $\vec{B}$ to $\vec{H}$ can be considered as linear. Finally, for isotropic loss-less materials the dielectric permittivity, Ɛ($\vec{r}$,w) is scalar and real, where $\vec{r}$is the spectral vector and Ɛ is the angular frequency of light. Then, the constitutive equations of the material are given by:

$$\mathbf{D}(\mathbf{r}, \mathrm{t}) = \varepsilon(\mathbf{r})\mathbf{E}(\mathbf{r}, \mathrm{t}) \tag{2.2a}$$

$$\mathbf{B}(\mathbf{r}, \mathrm{t}) = \mu_0 \mathbf{H}(\mathbf{r}, \mathrm{t}) \tag{2.2b}$$

Where μ_0 is the magnetic pemeability of vacuum. If harmonic time dependence of the electromagnetic fields is assumed, the fields can be written as:

$$\mathbf{E}(\mathbf{r},\mathrm{t}) = \mathbf{E}(\mathbf{r})\mathrm{e}^{\mathrm{j}\omega\mathrm{t}} \tag{2.3a}$$

$$\mathbf{H}(\mathbf{r},\mathrm{t}) = \mathbf{H}(\mathbf{r})\mathrm{e}^{\mathrm{j}\omega\mathrm{t}} \tag{2.3b}$$

So by using these following equation can be obtained

$$\nabla * \mathbf{E}(\mathbf{r}) = -\mathrm{i}\omega\varepsilon\mu_0\mathbf{H}(\mathbf{r}) \tag{2.4a}$$

$$\nabla * \mathbf{H}(\mathbf{r}) = \mathrm{i}\omega\varepsilon\mathrm{r}\mathrm{E}(\mathrm{r}) \tag{2.4b}$$

$$\nabla.\mathbf{H}(\mathbf{r}) = 0 \tag{2.4c}$$

$$\nabla.\varepsilon(\mathbf{r})\mathbf{E}(\mathbf{r}) = 0 \tag{2.4d}$$

Equation 2.2a and equation 2.2b can be rearranged into a single vectorial expression satisfied by the magnetic field $\vec{H}(\vec{r})$

$$\nabla * \frac{1}{\varepsilon(\boldsymbol{r})(\nabla * \boldsymbol{H}(\boldsymbol{r}))} = \omega^2\mu_o\boldsymbol{H}(\boldsymbol{r}) \tag{2.5}$$

This general expression represents an eigen value problem. If the spatial dependence of the dielectric medium whose dielectric constant of any medium is known, the solution to equation 2.5 will provide the solutions to the optical modes. However, the complex geometry of photonic crystals makes the solution of this equation non-trivial, and outside of the simplest cases, requires a fair amount of computational work to provide answers. The left side of the equation 2.2 can be formulated as an operator (Θ) acting on $\vec{H}(\vec{r})$ so that it takes explicitly the form of an eigen value problem.

$$\Theta\boldsymbol{H}(\boldsymbol{r}) = \omega^2\mu_o\boldsymbol{H}(\boldsymbol{r}) \tag{2.6a}$$

$$\Theta = \nabla * (\nabla * \frac{1}{\varepsilon(\boldsymbol{r})}) \tag{2.6b}$$

Similarly to equation 2.4, a master equation for $\vec{E}$ could also be formulated. However, it is more convenient to express the problem in terms of $\vec{H}(\vec{r})$. This is because the operator Θ is Hermitian which simplifies the computational problem. After obtaining the modes $\vec{H}(\vec{r})$ for

a given frequency, the following relation can be used to obtain the electric field distribution,

$$\boldsymbol{E}(\vec{r})=(-j/\omega\varepsilon(\vec{r}))\nabla*\vec{\boldsymbol{H}}(\vec{r}) \tag{2.7}$$

In optical fibers, the translational invariance of the refractive index profile along the z-directional leads to the following form of solutions.

$$\boldsymbol{H}(x,y,z)=\boldsymbol{H}(x,y)e^{-i\vec{\beta}\vec{z}} \tag{2.8}$$

When β is the propagation constant along z (the fiber axis). The harmonic mode $\vec{H}$(x,y) is the eigen vector associated to the eigen value β. In the case of a wave propagation in a homogeneous medium ($\varepsilon(\vec{r})$ = ε) equation [2.3] reduces to the Helmholtz equation, which can be solved in a closed form. In the same manner, if the geometry of the system is simple enough to apply analytical solution. This is the case of conventional step-index fibers. However, in the case of photonic crystal fibers the eigen value problem is more complicated due to the fibers complex geometry and analytical solutions are impossible to obtain. Powerful numerical methods are used to obtain the eigenvectors and Eigen values of the electromagnetic problem. Nevertheless, when analyzing infinite structures, the periodic nature of a photonic crystal allows the simplification of the electromagnetic problem to a small region of the photonic crystal.

Photonic crystals can be described in terms of a periodic array of points in space called a lattice, and a unit cell which is represented ideally at every point of the lattice. The unit cell is defined as the smallest area, which by mere translation can fully represent the structure. Every point of the lattice can be defined in terms of the lattice vectors ($\vec{\mu_1}\vec{\mu_2}\vec{\mu_3}$), which are the smallest vectors that can connect one lattice point with another. All crystals have an associated lattice in Fourier space called reciprocal lattice which consists of the set of all the allowed terms in the Fourier expansion of the periodic structure. The lattice is defined in terms of the primitive reciprocal lattice vectors ($\vec{g_1}\vec{g_2}\vec{g_3}$).

To examine the way a photonic crystal affects the propagation of light passing through it, the dielectric constant of the structure must be expressed in terms of the lattice vector$\vec{R}$. The periodic dielectric function of a photonic crystal satisfies

$$\varepsilon(\vec{r}) = \varepsilon(\vec{r}+\vec{R}) \tag{2.9}$$

According to Bloch's theorem the solution of the magnetic field can be expressed as Bloch's states consisting of a plane wave modulated by a periodic function with the same periodicity a photonic crystal.

$$\boldsymbol{H_K} = \overrightarrow{U_k}(\vec{r})e^{-i\vec{k}\vec{r}} \tag{2.10}$$

Where $\vec{k}$ is the wave vector, $\vec{r}$ denotes the position vector and $\overrightarrow{U_k}(\vec{r})$ has the same periodicity as the lattice, i.e. $\overrightarrow{U_k}(\vec{r}) = \overrightarrow{U_k}(\vec{r}+\vec{R})$. Therefore knowing the values of the magnetic field $\overrightarrow{H_k}$ in a unit cell, the magnetic field in all the structure can be inferred from equation 2.10. In other words, the electromagnetic problem in an infinite photonic crystal is reduced to finding the values of the magnetic field in a small area. In the same way, in the reciprocal lattice, a Blotch state for a wave vector $\vec{k}$ is equal to the Bloch state $\vec{k}+\vec{G}$ where $\vec{G}$ is any vector of the reciprocal lattice. This gives rise to a periodicity of the dispersion curve in the reciprocal space (or $\vec{k}$ space), expressed as $\omega(\vec{k}) = \omega(\vec{k}+\vec{G})$. Consequently, the dispersion information of the modes is contained in a region of the reciprocal space called the Brillouin zone and only wave vectors $\vec{k}$ lying inside the Brillouin zone identify an independent mode. Therefore the dispersion curves of photonic crystals are normally presented as plots of frequency versus wave vectors in the Brillouin zone.

2.4 Attenuation and Distortion in Optical Fiber

The attenuation or transmission loss of optical fibers has proved to be one of the most important factors in bringing about their wide acceptance in telecommunications. Since fibers are used to transport light over distances ranging from meters to thousands of kilometers, over such distances, even small imperfections can lead to substantial effects. Signal attenuation largely determines the maximum repeater-less separation between a

transmitter and a receiver. Since repeaters are expensive to fabricate, install, and maintain, the degree of attenuation in a fiber has a large influence on system cost. Of equal importance is the signal distortion. The distortion mechanisms in a fiber cause optical signal pulses to broaden as the travel along a fiber. If these pulses travel sufficiently far, they eventually overlap with neighboring pulses, thereby creating errors in the receiver output. The signal distortion mechanisms thus limit the information-carrying capacity of a fiber.

Fiber losses depend on the wavelength of transmitted light. The losses are considerably higher for shorter wavelengths and exceed 5 dB/km in the visible region, making it unsuitable for long-haul transmission. Several factors contribute to overall losses; their relative contributions are also shown in Fig. 2.2. However the common losses that affect the signal transmission are such as absorption, Rayleigh scattering, confinement loss, bend loss, dispersion and variations in the fiber structure along the length.

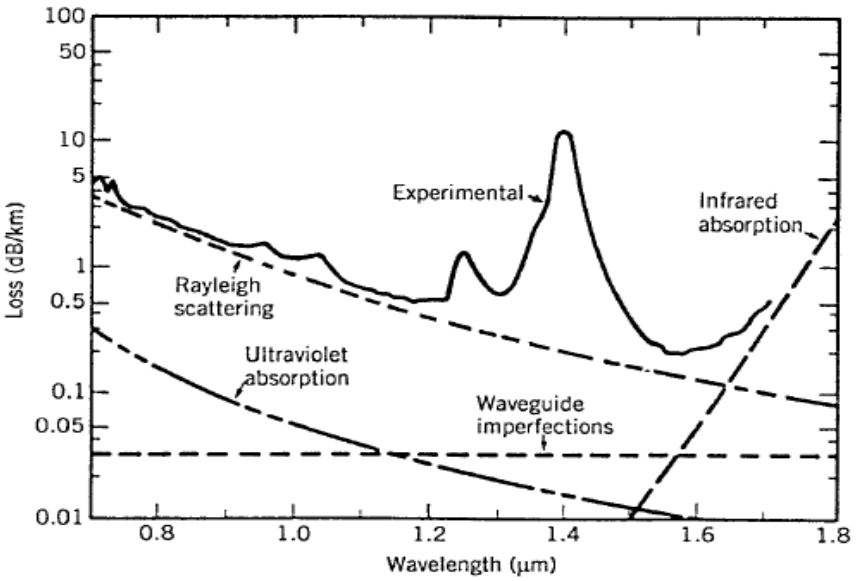

Fig. 2.2: Loss spectrum of single mode fiber produced in 1979 [1].

Fig. 2.2 depicts the loss spectrum $\alpha(\lambda)$ of a single-mode fiber made in 1979 with 9.4 μm core diameter, $\Delta = 1.9\times10^{-3}$,and 1.1 μm cutoff wavelength [1]. The fiber exhibited a loss of only about 0.2 dB/km in the wavelength region near 1.55 μm, the lowest value first realized in 1979.

2.4.1 Absorption Loss

Absorption is caused by three different mechanisms: Absorption by atomic defects in glass compositions, extrinsic absorption by impurity atoms in glass material and intrinsic absorption by the basic constituent atoms of the fiber material.

Material absorption is a loss mechanism related to the material composition and the fabrication process for the fiber, which results in the dissipation of some of the transmitted optical power as heat in the waveguide. The absorption of the light may be intrinsic (caused by the interaction with one or more of the major components of the glass) or extrinsic (caused by impurities within the glass). An absolutely pure silicate glass has little intrinsic absorption due to its basic material structure in the near-infrared region. However, it does have two major intrinsic absorption mechanisms at optical wavelengths which leave a low intrinsic absorption window over the 0.8 to 1.7 μm wavelength range, as illustrated in Fig. 2.3, which shows a possible optical attenuation against wavelength characteristic for absolutely pure glass.

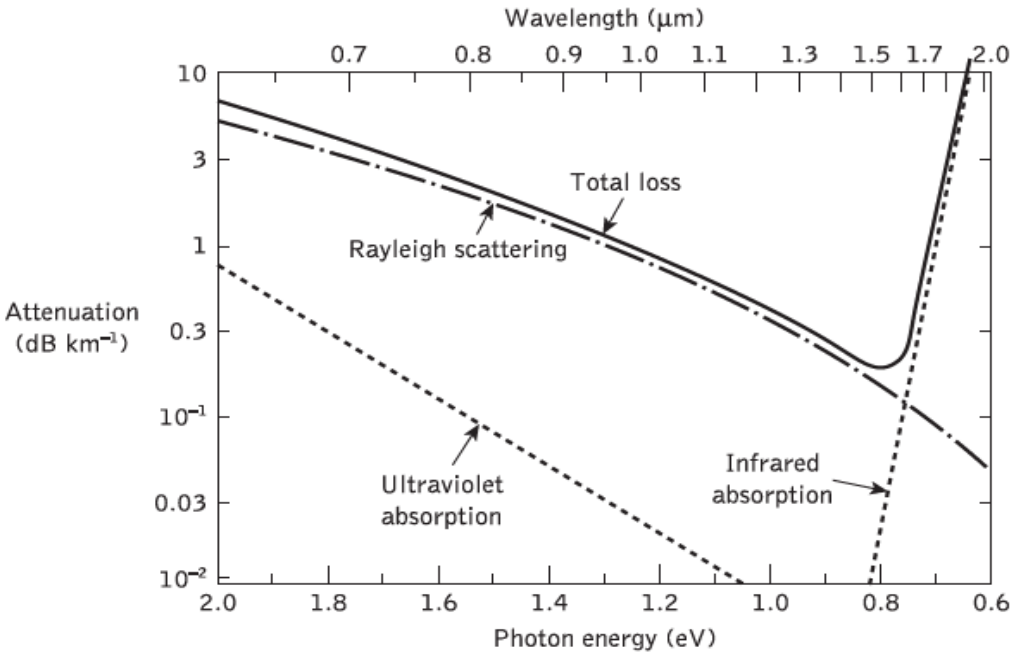

Fig. 2.3: Attenuation spectra for intrinsic loss mechanism [1].

The extrinsic absorption is basically caused by impurities in fiber materials. A major extrinsic loss mechanism is caused by absorption due to water (as the hydroxyl or OH ion) dissolved in the glass. These hydroxyl groups are bonded into the glass structure and have fundamental stretching vibrations.

2.4.2 Rayleigh Scattering

Rayleigh scattering is a fundamental loss mechanism arising from local microscopic fluctuations in density. Silica molecules move randomly in the molten state and freeze in place during fiber fabrication. Density fluctuations lead to random fluctuations of the refractive index on a scale smaller than the optical wavelength λ. Light scattering in such a medium is known as Rayleigh scattering. The scattering cross section varies as λ^{-4}. As a result, the intrinsic loss of silica fibers from Rayleigh scattering can be written as,

$$\alpha_R = C/\lambda^4 \tag{2.11}$$

where the constant *C* is in the range 0.7–0.9 (dB/km)-μm^4, depending on the constituents of the fiber core. These values of *C* correspond to α_R= 0.12–0.16 dB/km at λ=1.55μm, indicating that fiber loss in Fig. 2.2 is dominated by Rayleigh scattering near this wavelength.

Losses in hollow-core fibers are limited by the same mechanisms that limit loss in conventional fibers: absorption, Rayleigh scattering, confinement loss, bend loss and variations in the fiber structure along the length. However, these losses might be reduced below the levels found in conventional fibers because the majority of the light travels in the hollow core, in which scattering and absorption could be very low.

2.4.3 Confinement Loss

The presence of finite air holes in the core region causes leakage of optical mode from inner core region to outer air holes is unavoidable which results in confinement losses. The confinement loss of the fundamental mode is calculated from the imaginary part of the complex effective index n_{eff}, [12] using

$$Lc = 8.686 * K_0 Im[\eta_{eff}] \quad (2.12)$$

Where L_c is the confinement loss, K_0 is the free space wave number and $Im[\eta_{eff}]$ is the imaginary part of the effective refractive index.

The confinement loss in a photonic crystal fiber for single mode depends on the number of air holes in the structure greatly. The more the air holes, the more the loss reduces. This means that it is important to design such aspects of the PCF structure as air-holes diameter and hole-to-hole spacing, or pitch, in order to realize low-loss PCFs. In particular, the ratio between the air-hole diameter and the pitch must be designed to be large enough to confine light into the core. On the other hand, a large value of the ratio makes the PCF multi-mode. However, by properly designing the structure, the confinement loss of single mode PCFs can be reduced to a negligible level.

2.4.4 Bend Loss

Bends in the fiber constitute another source of scattering loss. Normally, a guided ray hits the core cladding interface at an angle greater than the critical angle to experience total internal reflection. However, the angle decreases near a bend and may become smaller than the critical angle for tight bends. The ray would then escape out of the fiber. In the mode description, a part of the mode energy is scattered into the cladding layer. The bending loss is proportional to exp (−R/Rc), where R is the radius of curvature of the fiber bend and Rc = a/(n_{21}−n_{22}). For single-mode fibers, Rc = 0.2–0.4 μm typically, and the bending loss is negligible (<0.01 dB/km) for bend radius R >5 mm. Since most macroscopic bends exceed R = 5 mm, macrobending losses are negligible in practice. A major source of fiber loss, particularly in cable form, is related to the random axial distortions that invariably occur during cabling when the fiber is pressed against a surface that is not perfectly smooth. Such losses are referred to as microbending losses. Microbends cause an increase in the fiber loss for both multimode and single-mode fibers and can result in an excessively large loss (~ 100 dB/km) if precautions are not taken to minimize them. For single-mode fibers, microbending losses can be minimized by choosing the V parameter as close to the cutoff

value of 2.405 as possible so that mode energy is confined primarily to the core. In practice, the fiber is designed to have V in the range 2.0 –2.4 at the operating wavelength.

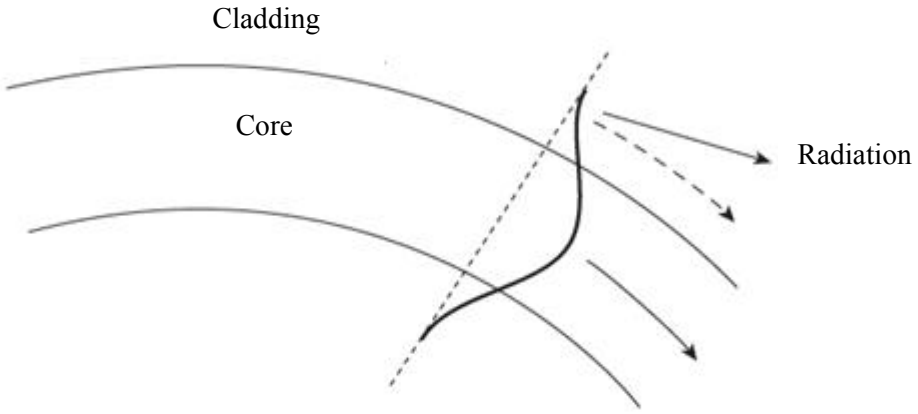

Fig. 2.4: Radiation loss at a fiber bend.

The part of the mode in the cladding outside the dashed arrowed line may be required to travel faster than the velocity of light in order to maintain a plane wave front. Since it cannot do this, the energy contained in this part of the mode is radiated away.

2.4.5 Dispersion

Dispersion of the transmitted optical signal causes distortion for both digital and analog transmission along optical fibers. When considering the major implementation of optical fiber transmission which involves some form of digital modulation, then dispersion mechanisms within the fiber cause broadening of the transmitted light pulses as they travel along the channel. The phenomenon is illustrated in Fig. 2.5, where it may be observed that each pulse broadens and overlaps with its neighbors, eventually becoming indistinguishable at the receiver input. The effect is known as inter-symbol interference (ISI). Thus an increasing number of errors may be encountered on the digital optical channel as the ISI becomes more pronounced. The error rate is also a function of the signal attenuation on the link and the subsequent signal-to-noise ratio (SNR) at the receiver. However, signal dispersion alone limits the maximum possible bandwidth attainable with a particular optical fiber to the point where individual symbols can no longer be distinguished.

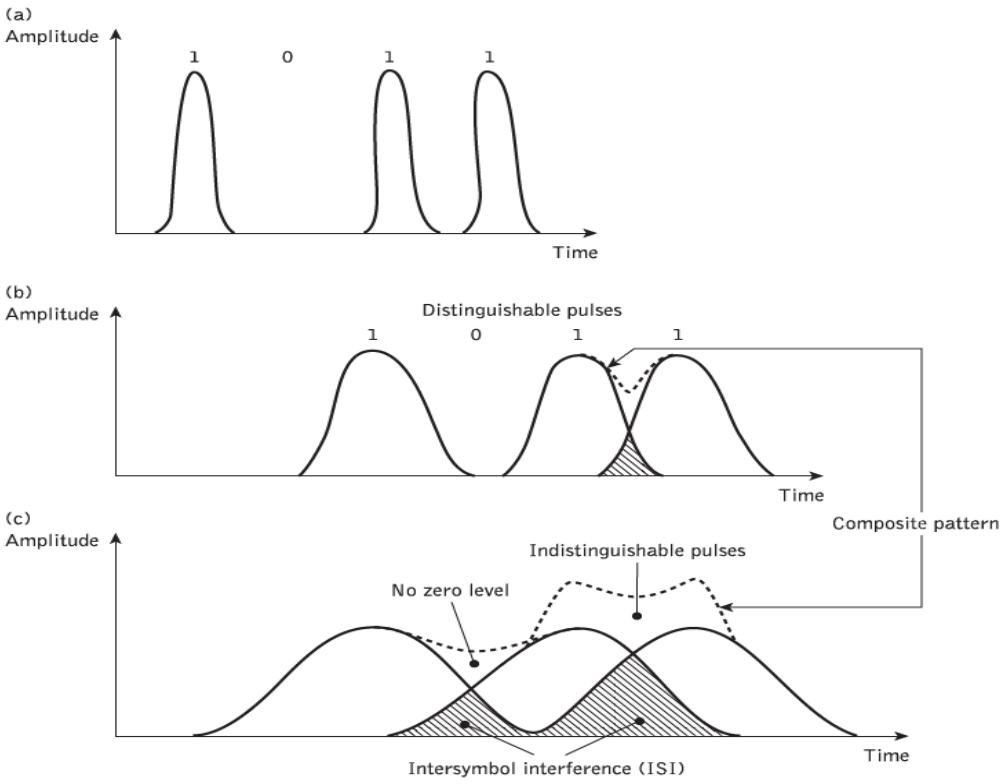

Fig. 2.5: (a) Light input of fiber (b) Light output at distance L_1 (c) Light output at distance L_2>L_1

Dispersion occurs in all types of fibers and is a result of finite spectral line width of optical source. The dispersion occurs within single mode is intramodal dispersion or chromatic dispersion and within multimode is intramodal dispersion.

2.4.5.1 Intramodal Dispersion

Chromatic dispersion is the variation in group velocity with a variation in wavelength. This variation in velocity results in broadening of pulses when traveling through the fiber, which overlap and result in increased bit error rate. Increase in bit error rate affects the signal quality. In high speed transmission, chromatic dispersion is a major limiting factor. It is a result of group velocity being a function of wavelength λ. The two main causes of intramodal dispersion are material dispersion and waveguide dispersion. The chromatic dispersion in PCF is given by

$$D(\lambda) = -(\frac{\lambda}{C})\,[d^2 Re(\eta_{eff})/d\lambda^2] \qquad (2.13)$$

Where c is the velocity of light and λ is the operating wavelength.

Pulse broadening due to material dispersion results from the different group velocities of the various spectral components launched into the fiber from the optical source. It occurs when the phase velocity of a plane wave propagating in the dielectric medium varies nonlinearly with wavelength, and a material is said to exhibit material dispersion when the second differential of the refractive index with respect to wavelength is not zero (i.e. $d_2n/d\lambda_2 \neq\neq 0$). The pulse spread due to material dispersion may be obtained by considering the group delay Tg in the optical fiber which is the reciprocal of the group velocity v_g.

The waveguiding of the fiber may also create chromatic dispersion. This results from the variation in group velocity with wavelength for a particular mode. Multimode fibers, where the majority of modes propagate far from cutoff, are almost free of waveguide dispersion and it is generally negligible compared with material dispersion.

2.4.5.2 Intermodal Dispersion

The intermodal dispersion (sometimes referred to simply as modal or mode dispersion) results from the propagation delay differences between modes within a multimode fiber. As the different modes which constitute a pulse in a multimode fiber travel along the channel at different group velocities, the pulse width at the output is dependent upon the transmission times of the slowest and fastest modes. Among the fiber types the multimode step index fibers exhibit a large amount of intermodal dispersion which gives the greatest pulse broadening. The overall pulse broadening in multimode graded index fibers is far less than that obtained in multimode step index fibers (typically by a factor of 100). Thus graded index fibers used with a multimode source give a tremendous bandwidth advantage over multimode step index fibers.

Under purely single-mode operation there is no intermodal dispersion and therefore pulse broadening is solely due to the intramodal dispersion mechanisms. In theory, this is the case with single-mode step index fibers where only a single mode is allowed to propagate. Hence they exhibit the least pulse broadening and have the greatest possible bandwidths, but in general are only usefully operated with single-mode sources.

2.5 Effective Mode Area

Effective area in a PCF is the area where light is confined in a fiber. In PCFs, the effective area includes the core region and a small fraction of areas in the cladding region. A_{eff} depends on various fiber parameters like the core radius and the core cladding index difference. The effective area increases with the increase in diameter of air holes in the cladding region in a PCF. The area is calculated by [11],

$$A_{eff}(\lambda) = \frac{\left[\int_{-\infty}^{\infty}\int_{-\infty}^{\infty}(|E(x,y)|^2)dxdy\right]^2}{\left[\int_{-\infty}^{\infty}\int_{-\infty}^{\infty}(|E(x,y)|^4)dxdy\right]} \tag{2.14}$$

where E is the electric field distribution derived by solving an Eigen value problem drawn from Maxwell's equations. Furthermore, in PCF nonlinearities come into action, when the effective mode area of propagation of light is very small. Nonlinearity depends on the nonlinear refractive index of the material. The larger the effective mode area is, the smaller the nonlinearity value is.

2.6 Birefringence

A single-mode fiber is not truly single mode because it can support two degenerate modes that are polarized in two orthogonal directions. Under ideal conditions, a mode excited with its polarization in the x direction would not couple to the mode with the orthogonal y-polarization state. In real fibers, small departures from cylindrical symmetry because of random variations in core shape and stress-induced anisotropy result in a mixing of the two polarization states by breaking the mode degeneracy. Mathematically, the mode propagation constant becomes slightly different for the modes polarized in the x and y directions. This property is referred to as modal birefringence. The strength of modal birefringence is defined as [14] ,

$$\beta_m = n_y - n_x \tag{2.15}$$

If an input pulse excites the two polarization components, the two components travel along the fiber at different speeds because of their different group velocities. The pulse becomes broader at the output end because group velocities change randomly in response to random

changes in fiber birefringence. This phenomenon, referred to as polarization-mode dispersion (PMD).

2.7 Nonlinear Coefficient

The nonlinear coefficient (γ) in a PCF can be calculated by [14],

$$\gamma = \frac{2\pi n_2}{\lambda A_{eff}} \tag{2.16}$$

Where n_2 is nonlinear refractive index, the value of which is 2.66×10^{-20} W/m. Enhanced nonlinearity can be achieved by the use of different materials and different structures of PCF. In photonic crystal fiber nonlinearities come into action, when the effective mode area of propagation of light is very small. Nonlinearity depends on the nonlinear refractive index of the material. The larger the effective mode area is, the smaller the nonlinearity value is. Certain materials like soft-glass and chalcogenide exhibit large value of nonlinearity.

2.8 Conclusion

Fiber losses are considerably higher for shorter wavelengths. The bandwidth of the fiber is limited by signal dispersion within the fiber, which determines the number of bits of information transmitted in a given period of time. The attenuation or transmission loss of optical fibers has proved to be the most important factors in bringing about their wide acceptance in telecommunication. A number of mechanisms are responsible for the signal attenuation within optical fibers. These mechanisms are influenced by material composition, preparation and waveguide structure. Confinement losses can be eliminated by forming a sufficiently thick cladding.

CHAPTER 3

ANALYSIS OF THE PCF SYSTEM MODELS

3.1 Introduction

Till now, several designs for PCFs' have been proposed to achieve a very low chromatic dispersion and low confinement loss. Various designs such as different core geometries and multiple air-hole diameters in different rings have been studied to achieve these characteristics over a wide wavelength range. However, by suitably choosing physical parameters like diameter of the air holes, shape of holes, number of holes in the area surrounding the core, spacing between adjacent air holes PCFs could be designed with desired properties. In this analysis, a hexagonal, octagonal and decagonal shaped PCF with identical design parameters are considered. A new index guiding hybrid photonic crystal fiber (Hy-PCF) is also designed. COMSOL Muti-Physics 4.4 has been used as the modeling and simulation tool where the optical mode analysis is done by the electromagnetic module.

3.2 System Model

3.2.1 System Diagram

The geometrical model of the designed hexagonal, octagonal, decagonal and hybrid PCF is shown in Fig. 3.1, Fig. 3.2, Fig. 3.3 and Fig. 3.4 respectively.

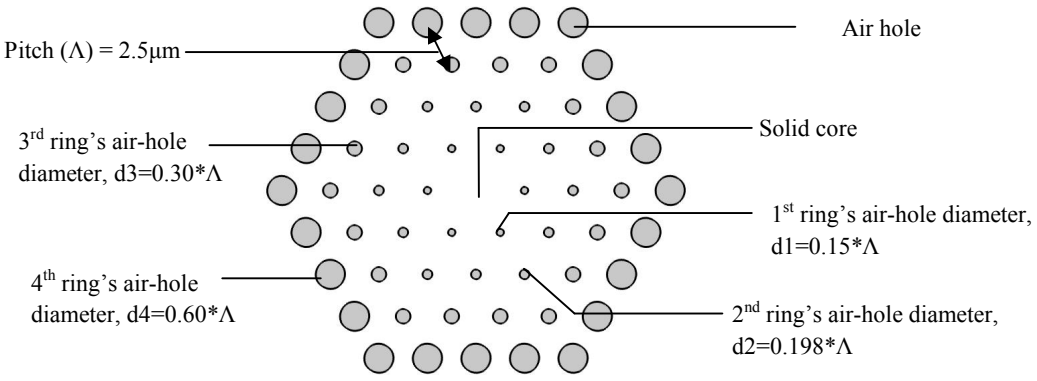

Fig. 3.1: System model of the H-PCF

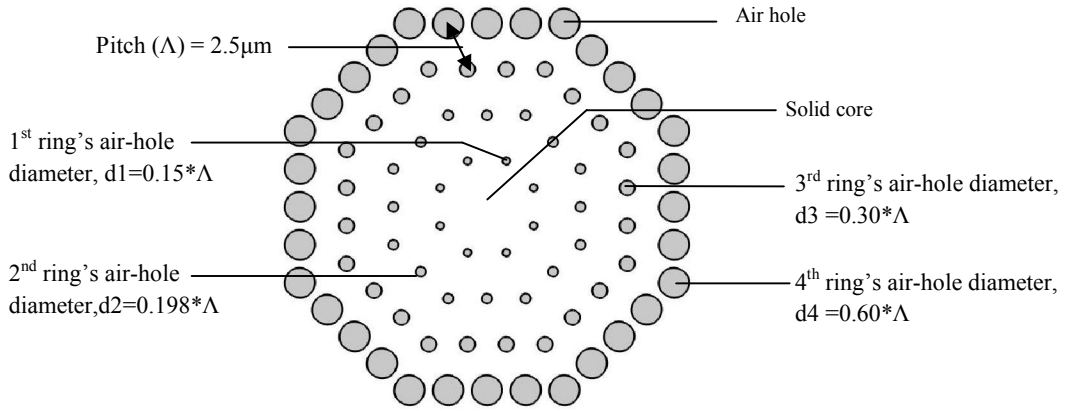

Fig. 3.2: System model of the O-PCF

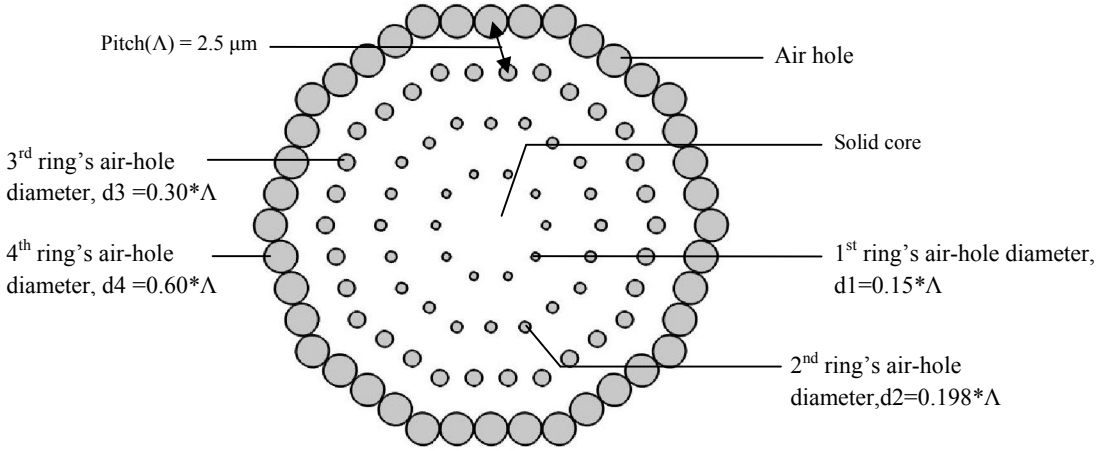

Fig. 3.3: System model of the D-PCF

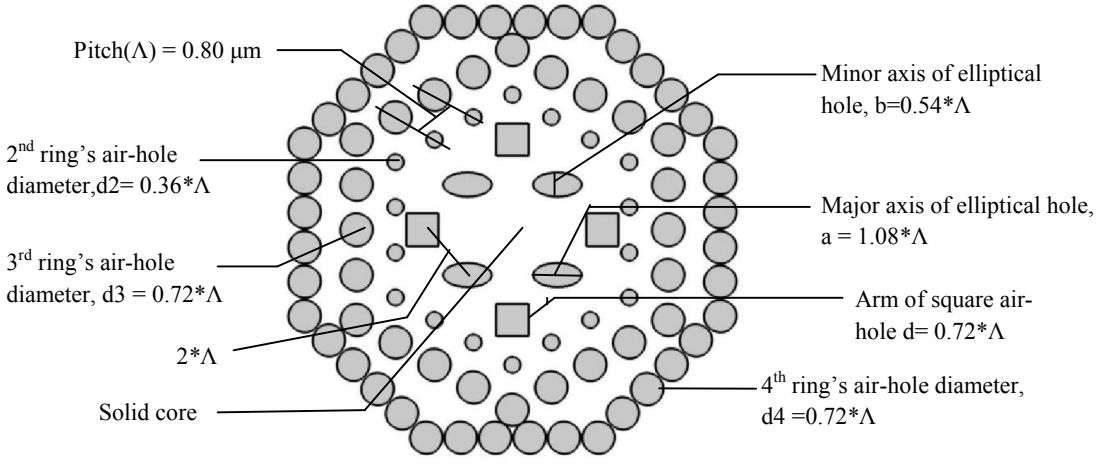

Fig. 3.4: System model of the Hy-PCF

3.2.2 Description of the System Model

The fiber material is pure silicon dioxide (SiO_2) in the core and cladding regions. The same material is chosen for the Perfectly Matched Layer (PML). But due to the present of air holes, the refractive index of cladding becomes lower than the core. This is very important in solid-core PCFs to get better dispersion characteristics. The choice of larger air holes in the outer rings helps to achieve low confinement loss. In cladding, the air holes are distributed in four rings. The distance between any two adjacent air-hole rings is called pitch (Λ).

The pitch for hexagonal, octagonal and decagonal structure is chosen as 2.5 μm. The diameter of air holes in most outer ring (4^{th} ring) is chosen as d4 = 0.60*Λ μm. In 3^{rd}, 2^{nd} and 1^{st} ring around the core, the diameters are 0.30*Λ, 0.198*Λ and 0.15*Λ respectively. The total number of air holes in 1^{st}, 2^{nd}, 3^{rd}, 4^{th} ring is 6, 12, 18 and 24 respectively in hexagonal structure (H-PCF). In octagonal (O-PCF) and decagonal structure (D-PCF) these are 8, 16, 24, 32 and 10, 20, 30, 40 respectively.

The geometry of the Hy-PCF also consists of four air-hole rings. Among them the first one around the core is square shaped and comprised of four square shaped and four elliptical shaped air holes. The arm of a square hole is d = 0.72*Λ μm and the major axis and minor axis of each elliptical hole is of a = 1.08*Λ μm and b = 0.54*Λ μm respectively. The next two air-hole rings are hexagonal and in the most outer ring air-holes are distributed in octagonal shaped arrangement. Only circular air holes are used in these three rings. The diameter of air holes in second ring is d2 = 0.36*Λ μm and in third and fourth ring is d3 = d4 = 0.72*Λ μm. Λ is chosen as 0.80 μm in this case. The total numbers of air holes in 1^{st}, 2^{nd}, 3^{rd}, 4^{th} rings are 8, 18, 24 and 40 respectively.

Solid core makes the wave propagation characteristics fixed, for a particular set of parameters, whereas we can modify the electric field and hence the optical wave propagation characteristics by changing different parameters at different times.

3.2.3 Electric Field Distribution

Electric field distribution, E is derived by solving an Eigen value problem drawn from Maxwell's equation. It is known that, in the best ray passing model, the light is strongly confined in the central core region, i.e. the central core region has the highest magnetic field density for a specific model. In order to find the best possible outcome the resultant effective mode index has changed for a given wavelength and find which has most of the light passing through the central region and thus find the desired value of effective mode index for any wavelength. The COMSOL Multi-physics software provides a numerical technique to simulate the electric field using the finite element method (FEM). The electric field intensity and distribution can be visualized using the FEM calculation with practical dimensions and material properties of the electro-spinning setup.

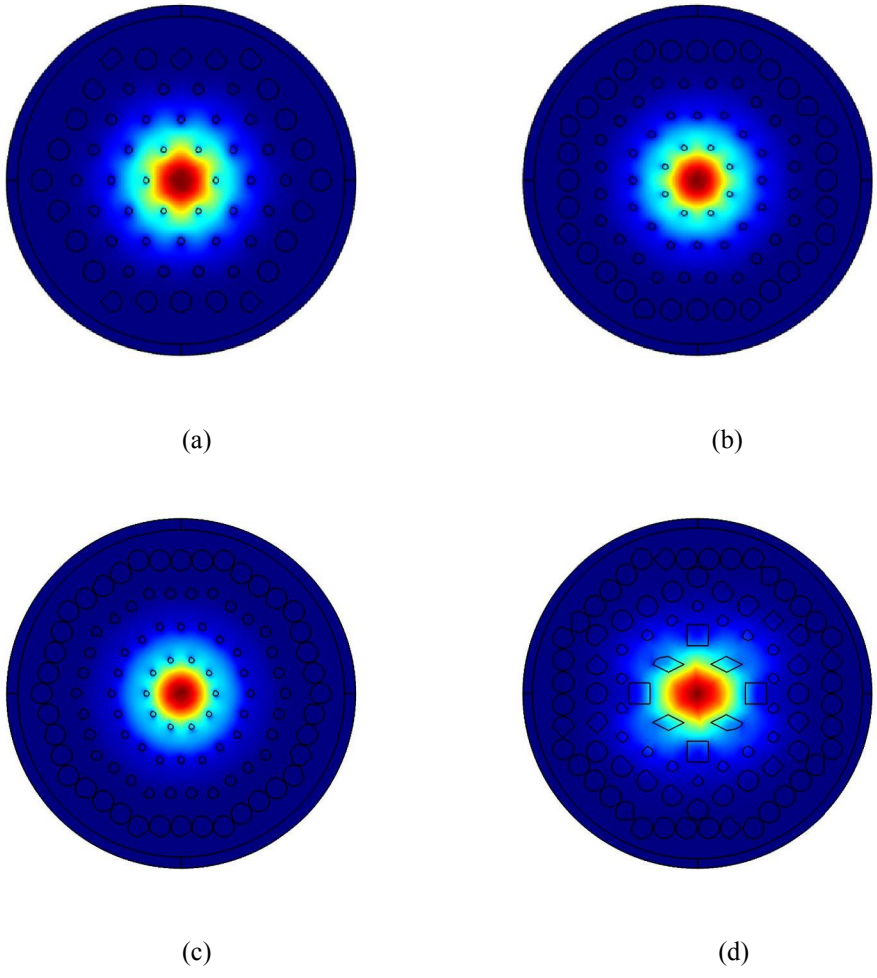

Fig. 3.5: Electric field distribution of (a) H-PCF, (b) O-PCF, (c) D-PCF and (d) Hy-PCF.

In Fig. 3.5 the Electric Field Distribution of different PCF structures are shown for 1.55 μm wavelengths. It is seen from the figure that the PCFs have strongly confined electric field in the core. The D-PCF has provided the finest light confinement and consequently the confinement loss achieved by it is the least. The loss behavior is discussed in the next chapter.

In Fig. 3.6 the 3-D electric field distribution or power intensity profiles of the PCFs are shown for 1.55 μm wavelengths. It is found that the peak value of the intensity lies at the center of the core. It also means that the PCFs have confined the electric field strongly to the core. As observed from the plot information, among four PCFs the power flow is highest in decagonal PCF and lowest in the hybrid PCF.

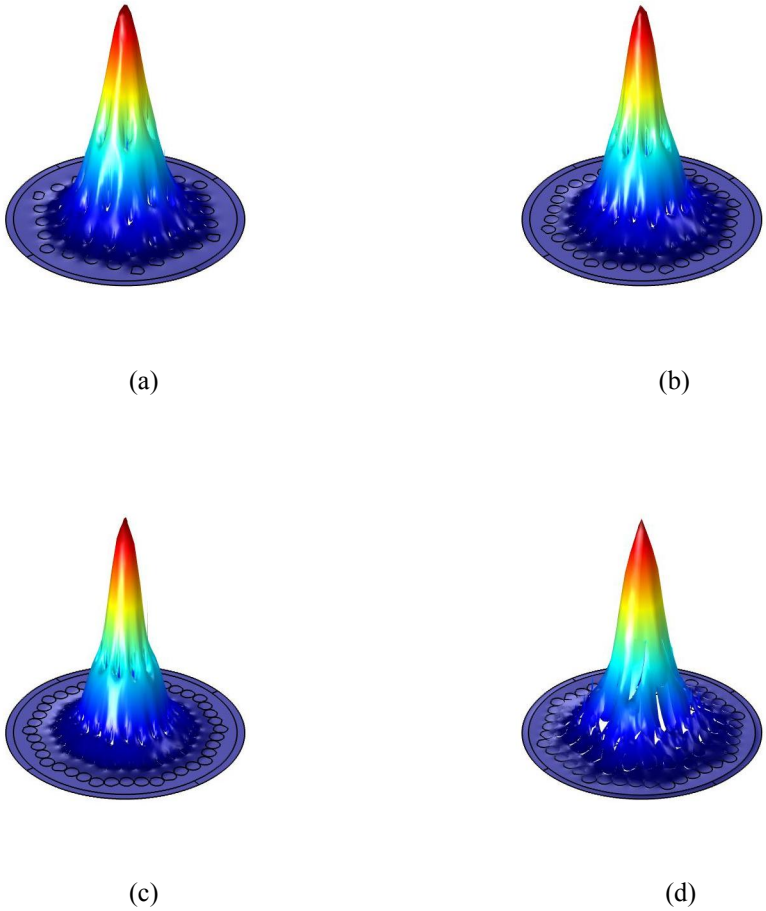

Fig. 3.6: 3-D electric field distribution of (a) H-PCF, (b) O-PCF, (c) D-PCF and (d) Hy-PCF at 1.55 μm

3.3 Conclusion

The detail description of the PCF models has provided the clear idea about the designed PCF structures and their geometrical properties. From the mode profiles of the PCFs, it is observed that the peak value of intensity lies at the centre of the core, which proves that the PCFs can confine the electric field strongly.

CHAPTER 4

RESULTS AND DISCUSSION

4.1 Introduction

COMSOL Multi-physics 4.4 simulation software is chosen as simulation tool and its full vector finite element method (FEM) is used for the modal analysis of the designed PCFs. The optical pulse propagating properties, such as dispersion, confinement loss, effective mode area, birefringence and nonlinear parameter are investigated using their respective formulas described in chapter 2. The effects of changing the shapes of PCF are analyzed to suggest a suitable PCF structure. A Hy-PCF shape is also analyzed to compare its characteristics with other designed models. The results are plotted graphically using MATLAB. In this chapter, the necessary data tables for sets of different parameters and plots are discussed and matched with their relevant theories described in chapter 2.

4.2 Analysis of Effective Mode Index Against Wavelengths

The values of effective mode index (η_{eff}) for the designed structures are determined from COMSOL. The plot of real part of effective mode index against wavelength for the three conventional structures is shown in Fig. 4.1.

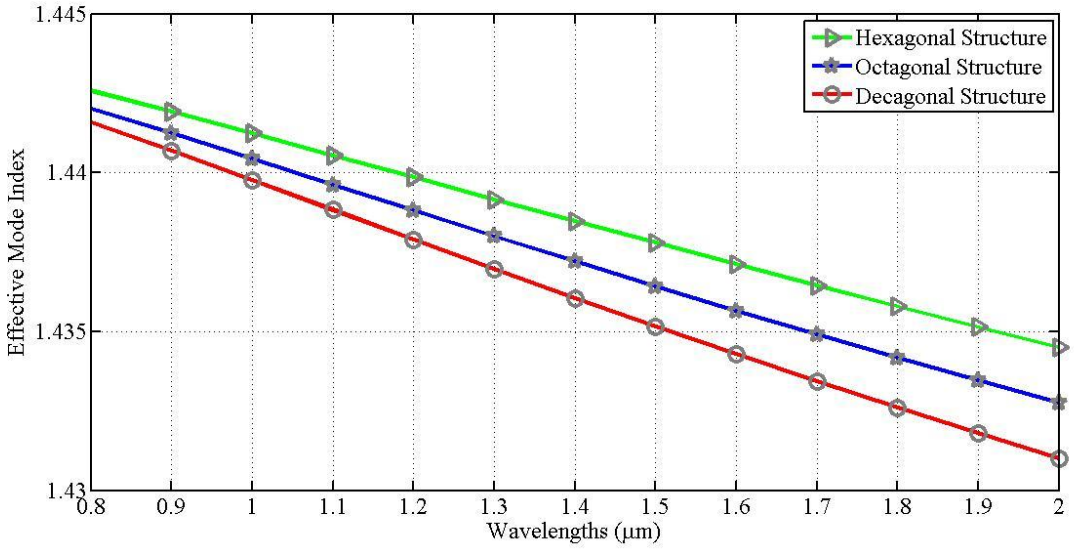

Fig. 4.1: Effective mode index against wavelength plot for three conventional structures

It is seen from the figure that with the effective mode index shows linear relationship with wavelengths for all the described structures. The analysis is made for 0.80 µm to 2.00 µm wavelengths. At lower wavelengths the difference among the value for different structures is less than those for higher wavelengths. The H-PCF is showing the highest effective mode index whereas the D-PCF is providing the lowest value. The O-PCF is midst of them. At 1.31µm wavelengths, real value of refractive index of H-PCF, O-PCF and D-PCF is 1.439154, 1.437992 and 1.436965 respectively. Further at 1.55 µm, the values become 1.437447, 1.436029 and 1.434719 respectively. Therefore it is seen that the effective mode index is decreasing with the increase of wavelengths.

In Fig. 4.2 the plot of effective mode index for the hybrid structure (Hy-PCF) is shown along with the decagonal structure (D-PCF). The D-PCF has the lowest mode index value among the three conventional PCF structures. But it is seen from Fig. 4.2 that the effective mode index value of Hy-PCF is much lower than that for the D-PCF. Its relationship with wavelengths for the Hy-PCF is linear too. But effective mode index decreases more rapidly with increase in wavelengths for Hy-PCF than D-PCF.

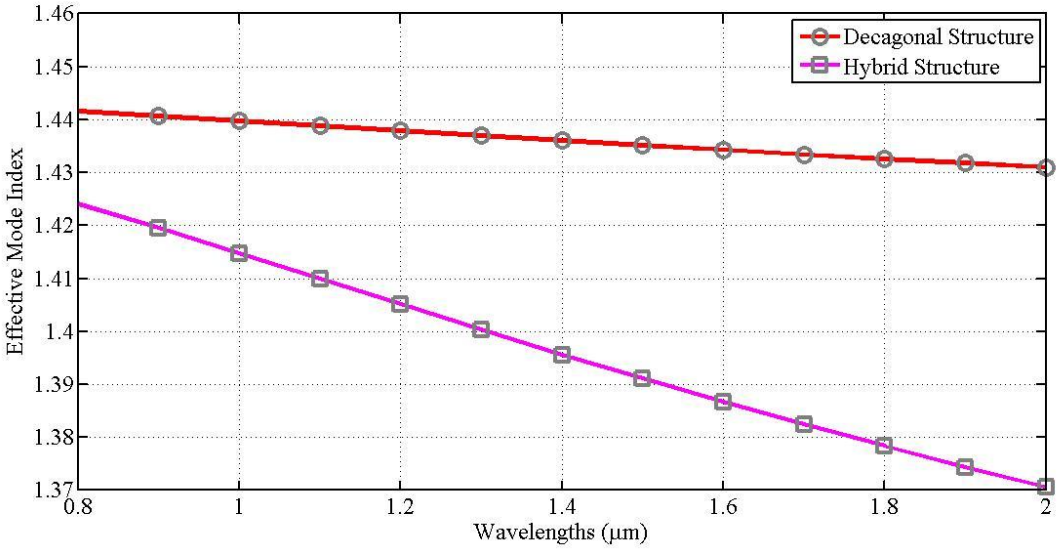

Fig. 4.2: Comparison of the real part of effective mode index curves between hybrid and decagonal structure against wavelength

4.3 Analysis of Dispersion Against Wavelengths

Dispersion is calculated from the real part of effective mode index by using equation (2.13). In Fig. 4.3 the dispersion characteristics of hexagonal structure is shown. It is seen from the figure that from 0.80 μm to 1.20 μm wavelengths dispersion is linearly decreasing with increase in wavelengths. In between 1.20 -1.80 μm wavelengths range the dispersion profile is varying in nature. Afterwards the curve is linearly increasing with wavelengths. The lowest −9.333 ps/nm-km dispersion is obtained at 1.40 μm. In 1.60-1.80 μm range dispersion curve has remained almost flattened with average −5 ps/nm-km value. At 0.85 μm, 1.31 μm and 1.55 μm the values are 6.69 ps/nm-km, −0.5421 ps/nm-km and −2.80 ps/nm-km respectively.

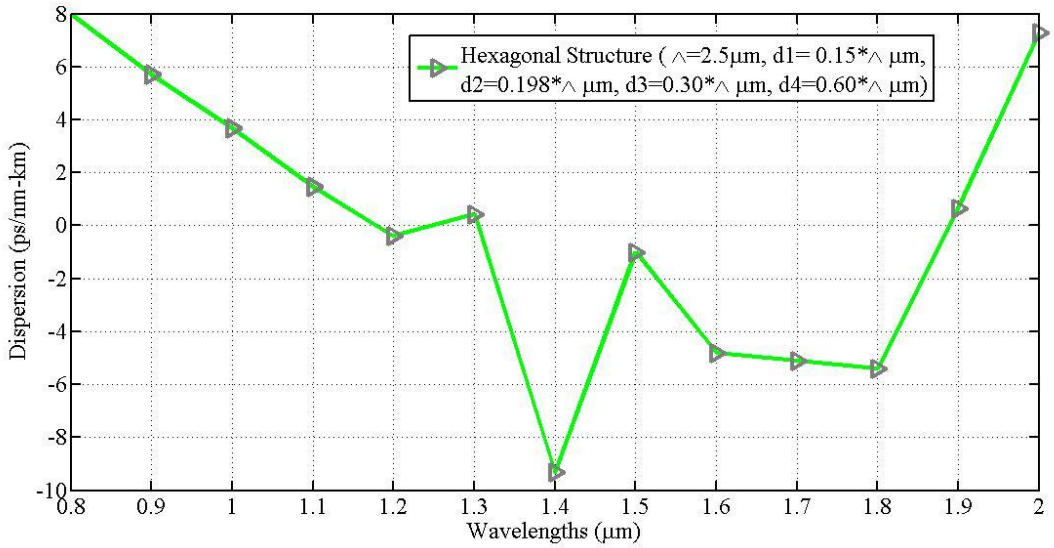

Fig. 4.3: Dispersion against wavelengths plot for the hexagonal PCF

In Fig. 4.4 the dispersion characteristics of octagonal structure is shown against wavelengths. It is seen that in 0.80-1.60 μm wavelength range the dispersion curve is almost linearly decreasing with increasing wavelengths. In 1.60-1.80 μm range dispersion curve is flattened just like in H-PCF. After that the value is linearly decreasing again. Dispersion is positive with 8.059 ps/km-nm value at 0.85 μm. At 1.31 μm only −5.40 ps/nm-km dispersion is seen. Dispersion has become more negative in third optical window where it is −8.61 ps/nm-km for 1.55 μm wavelengths.

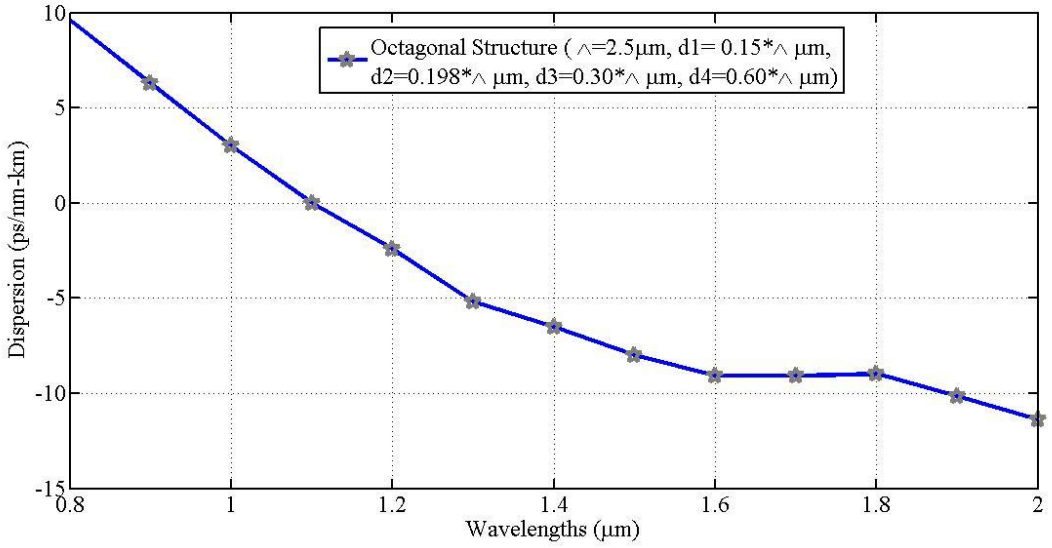

Fig. 4.4: Dispersion against wavelength plot for the octagonal PCF

The dispersion profile of decagonal structure is shown in Fig. 4.5.

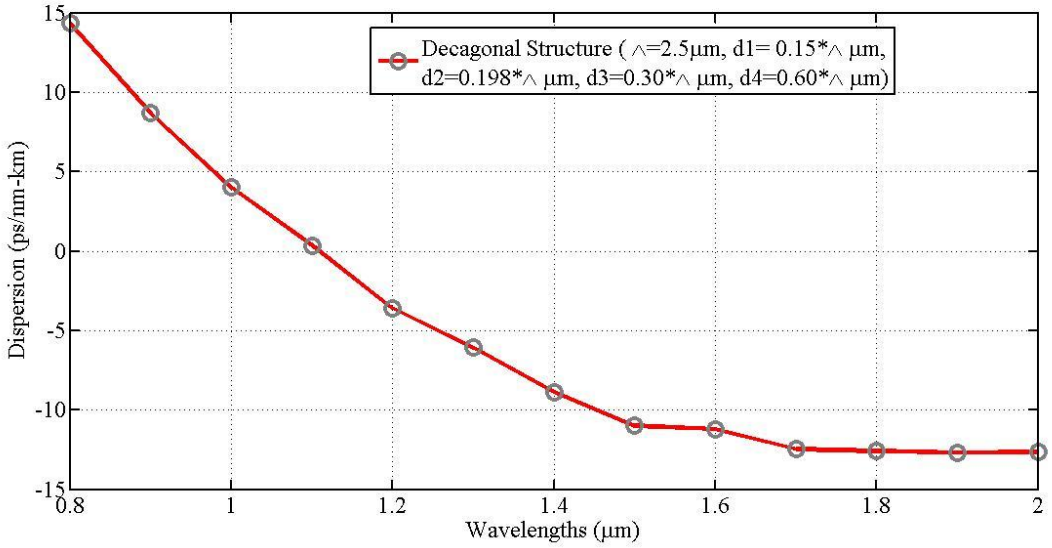

Fig. 4.5: Dispersion against wavelength plot for the decagonal structure.

It is seen from the figure that this structure is providing more positive dispersion at 0.85 µm wavelengths than the previous cases. But the value is not more than 15 ps/km-nm as per the observation. The curve is almost linearly decreasing with increasing wavelengths till 1.50 µm. But in the most desired optical window (1.50-1.60 µm) dispersion curve is flattened.

At 1.55 μm wavelengths −11 ps/nm-km dispersion is obtained. The value has decreased a little after that but became flattened again over 1.70 μm with average −12.6 ps/nm-km value. Overall the dispersion curve has varied in between +/−15 ps/km-nm range. A comparison among these three dispersion characteristics is seen in Fig. 4.6 below. It clarifies that the dispersion profile of H-PCF is quite varying whereas the O-PCF and D-PCF has shown almost linear characteristics. Over 1.80 μm dispersion is increasing in H-PCF but decreasing in others. The dispersion values are little more in D-PCF but below +/−15 ps/nm-km in three popular optical fiber transmission windows. In spite of having varying dispersion profile the H-PCF can be used in zero-dispersion applications for 1.31 μm wavelengths region due to its negligible dispersion value (−0.5421 ps/nm-km).

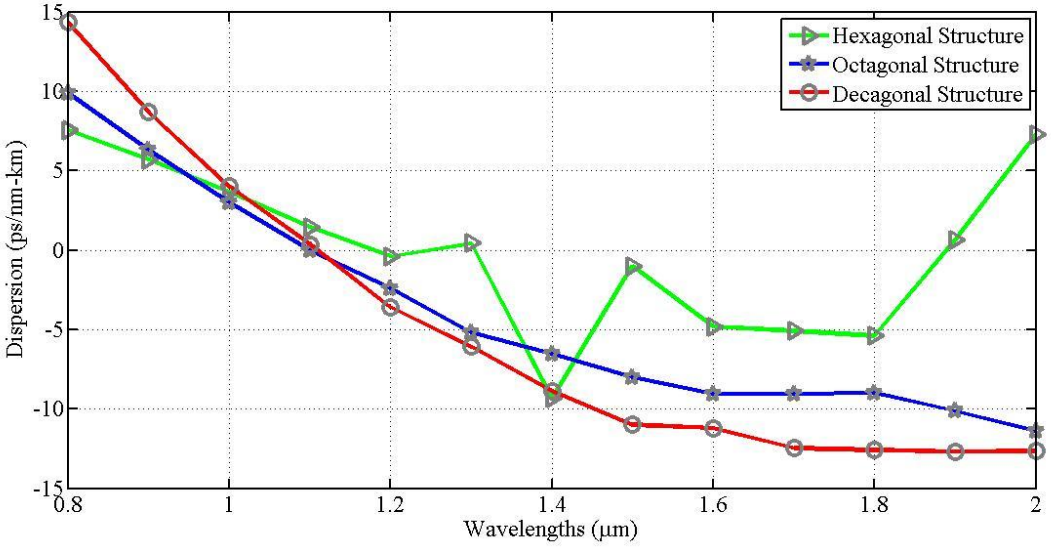

Fig. 4.6: Comparison of dispersion characteristics among three conventional structures

The dispersion vs. wavelengths curve for the hybrid PCF is shown Fig. 4.7 below along with the dispersion curve of D-PCF. It is seen that introduction of hybrid structure has provided more negative dispersion than that for the conventional structures. This curve is also linearly decreasing with increasing wavelengths like those for the O-PCF and D-PCF. Though it has provided large positive dispersion in wavelengths of first optical transmission window, the results are quite satisfactory for second and the most desired third optical window. At 1.31 μm the value is almost −40 ps/nm-km. The value has reached to −81.08 ps/nm-km at 1.55μm. So it can be stated that the hybrid structure is more suitable for

dispersion compensation technique where the conventional structures are suitable for obtaining near to zero dispersion value.

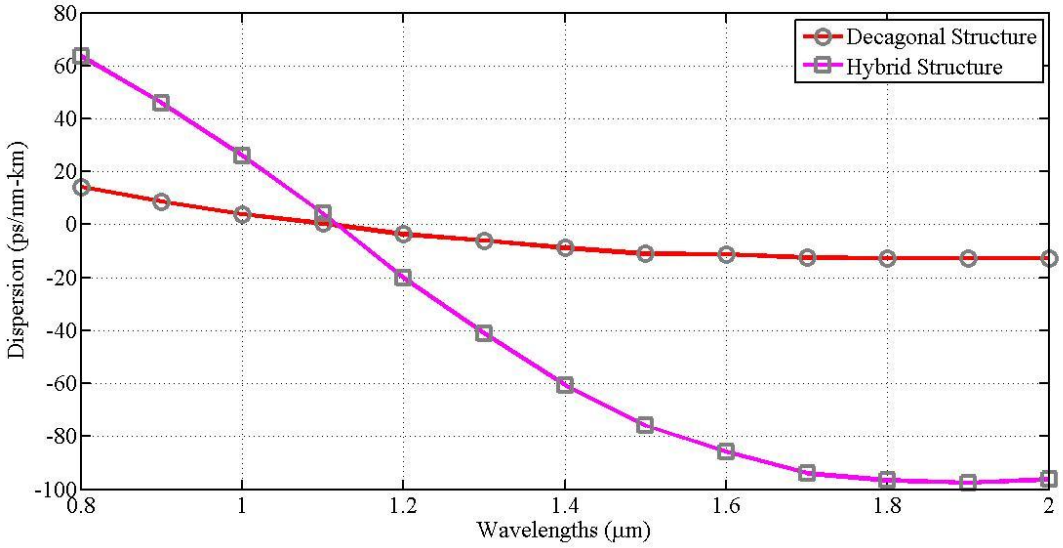

Fig. 4.7: Dispersion against wavelength plot for the Hy-PCF along with the D-PCF

4.4 Analysis of Confinement Loss Against Wavelengths

The confinement loss is obtained from equation (2.12) where the imaginary part of effective mode index is used. In Table 4.1 the confinement loss values of hexagonal, octagonal, decagonal and hybrid PCF structures are shown with an aim to compare their loss behavior.

Table 4.1: Confinement loss of H-PCF, O-PCF, D-PCF and Hy-PCF

Wavelengths (λ) (μm)	Confinement Loss (dB/m) for Different Structures			
	Hexagonal	Octagonal	Decagonal	Hybrid
1.50	0.417×10^{-6}	0.228×10^{-8}	0	0.023×10^{-4}
1.60	0.645×10^{-6}	0.519×10^{-8}	0	0.066×10^{-4}
1.70	0.985×10^{-6}	1.124×10^{-8}	2.207×10^{-9}	0.170×10^{-4}
1.80	1.486×10^{-6}	2.320×10^{-8}	3.442×10^{-9}	0.391×10^{-4}
1.90	1.606×10^{-6}	4.580×10^{-8}	5.269×10^{-9}	0.820×10^{-4}
2.00	1.983×10^{-6}	8.671×10^{-8}	7.927×10^{-9}	1.586×10^{-4}

The confinement loss of D-PCF is the lowest among all the described structures and this value is in the order of 10^{-9}. In case of D-PCF, before 1.70 μm the imaginary value of effective refractive index is so small that it cannot be determined due to software limitation. Consequently the confinement loss before 1.70 μm could not be calculated. Thus it is seen that the loss is in so negligible amount for D-PCF. The confinement loss of O-PCF is in the order of 10^{-8}, which can be neglected too. H-PCF has shown confinement loss behavior with 10^{-6} order, but the hybrid PCF is providing the highest loss value with order of 10^{-4}. This value is not negligible but can be considered reviewing the other benefits of this structure like high negative dispersion.

In Fig. 4.8 the confinement loss characteristics of H-PCF plotted against wavelengths is shown.

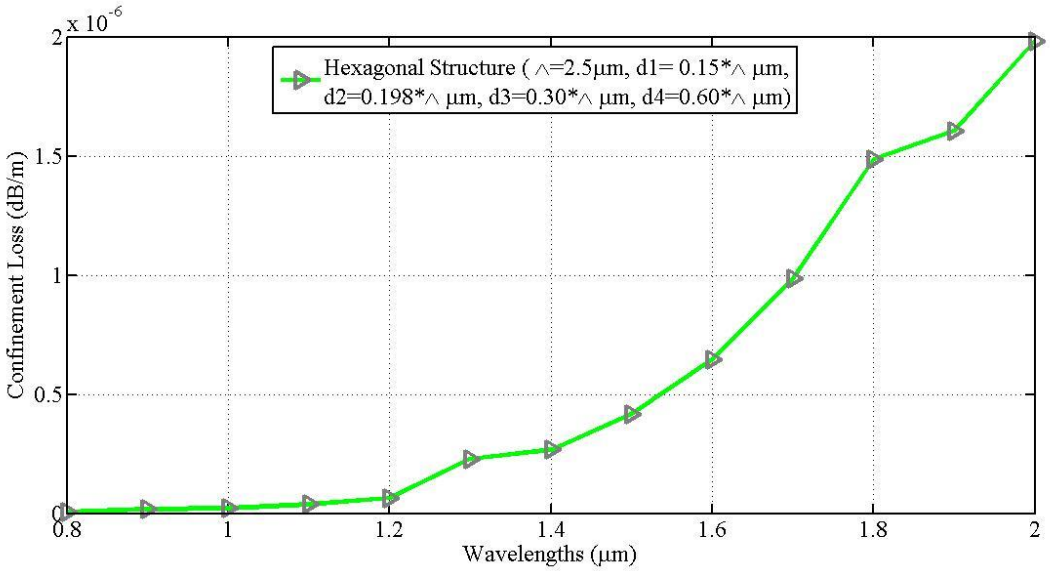

Fig. 4.8: Confinement loss characteristics of proposed H-PCF

It is seen from the figure that upto 1.20 μm wavelengths the variation in confinement loss against wavelengths is negligible. Afterwards the values are increasing more rapidly with increase in wavelengths. At 1.55 μm only 0.55×10^{-6}dB/m loss is obtained whereas at 850 μm it is almost zero. The confinement loss behavior of O-PCF and D-PCF is shown in Fig. 4.9 and Fig. 4.10 respectively.

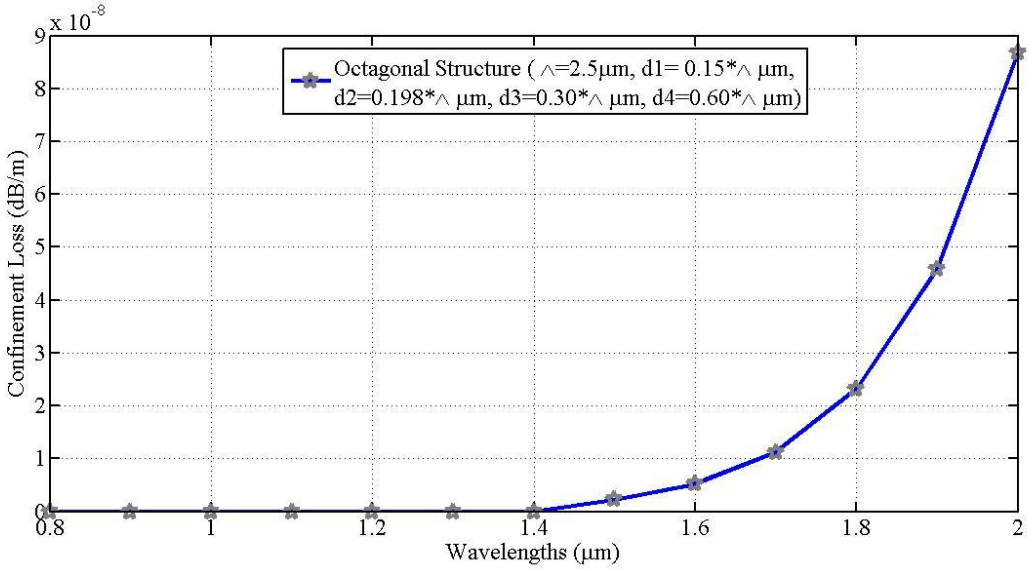

Fig. 4.9: Confinement loss characteristics of O-PCF

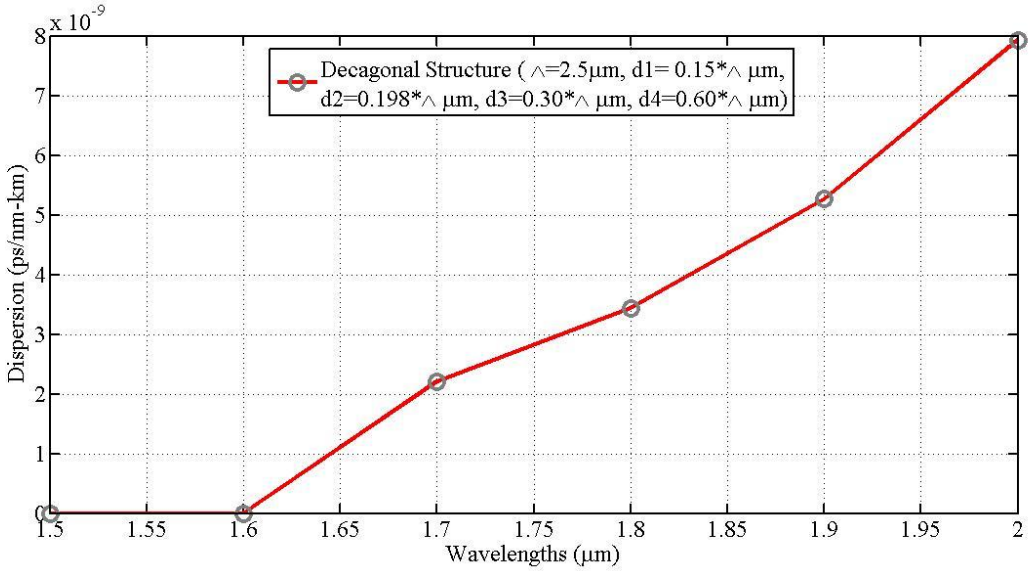

Fig. 4.10: Confinement loss characteristics of D-PCF

From the figures it is seen that the designed structures have exhibited a negligible confinement loss in a long wavelength range. Nearly zero confinement loss is achieved for O-PCF and D-PCF for the most interested region of optical fiber communication, i.e. 1.50 µm to 1.80 µm. The loss pattern of O-PCF is exponential whereas loss pattern of D-PCF is almost linearly increasing with wavelengths. The confinement loss characteristics of the hybrid structure against wavelengths are shown in Fig. 4.11

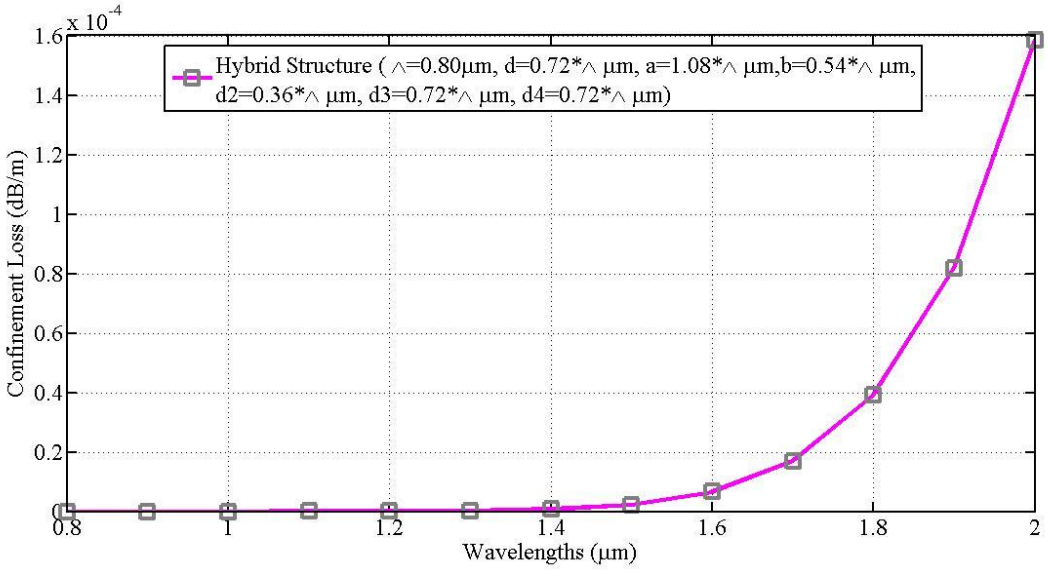

Fig 4.11: Analysis of confinement loss against wavelength for hybrid structure

It is seen from the figure that more loss is obtained from hybrid structure compared to the conventional PCFs. The loss is exponentially increasing with wavelengths. Though the loss value is larger than the conventional structures, the performance of other properties is better in Hy-PCF. Thus this structure can be suitable for the application of those properties ignoring its confinement loss.

4.5 Analysis of Effective Mode Area Against Wavelengths

For the calculation of effective mode area (A_{eff}), the corresponding terms of equation (2.14) is evaluated from derived values subsection of COMSOL. The values are plotted against wavelengths in Fig. 4.12 for the four designed structures. From the figure it is seen that the effective mode areas are linearly increasing with wavelengths. The hexagonal structure is exhibiting highest A_{eff} among all the four structures. The values of A_{eff} for octagonal and decagonal structure are close to that for the hexagonal. At 1.55 μm wavelengths the H-PCF, O-PCF and D-PCF have provided 25.42 μm^2, 19.83 μm^2 and 15.7 μm^2 effective mode areas respectively, whereas at 1.31 μm they are 35.31 μm^2, 29.4 μm^2, 25 μm^2 respectively. In case of the hybrid structure A_{eff} is much small with maximum 8.503 μm^2 only. The large effective area helps to reduce the effect of non-linear impairments on different PCF structures.

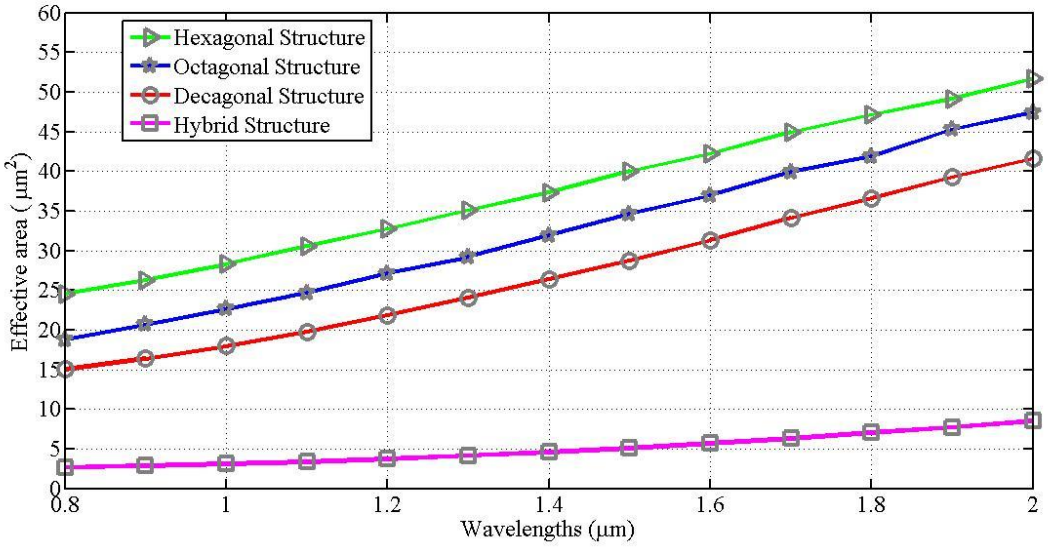

Fig. 4.12: Analysis of effective mode area against wavelength for different structures.

4.6 Analysis of Non Linear Coefficient Against Wavelengths

The nonlinear coefficients (γ) of the respective structures are calculated from equation (2.16). From the equation it is seen that the nonlinearity depends on the effective mode area and nonlinear refractive index of the material. Since in this case the value of nonlinear refractive index is kept fixed, the value of γ is depending on only the effective mode area. The relationship between effective mode area and nonlinear coefficient is inversely proportional. Consequently for higher values of effective mode area small nonlinearity is obtained and vice versa.

In Fig. 4.13 the values of nonlinear coefficient are plotted against wavelengths for the three conventional PCF structures. From the plots, it is seen that in case of three conventional structures of similar parameters the values of nonlinear coefficient are close to each other. At 0.85 μm wavelengths the value of γ for D-PCF, O-PCF and H-PCF are around 7.38$W^{-1}km^{-1}$, 9.32$W^{-1}km^{-1}$ and 11.79$W^{-1}km^{-1}$ respectively. This tells that for 0.85 μm the variation of γ among the conventional structures is only about +/−2$W^{-1}km^{-1}$. At 1.31 μm the values decreases to 4.98$W^{-1}km^{-1}$, 4.092$W^{-1}km^{-1}$ and 3.39$W^{-1}km^{-1}$ for the respective structures. Then at 1.55 μm the variation becomes only about +/−0.4$W^{-1}km^{-1}$. The corresponding

values of γ are $3.43W^{-1}km^{-1}$, $2.865W^{-1}km^{-1}$ and 2.493 $W^{-1}km^{-1}$ respectively for this wavelength.

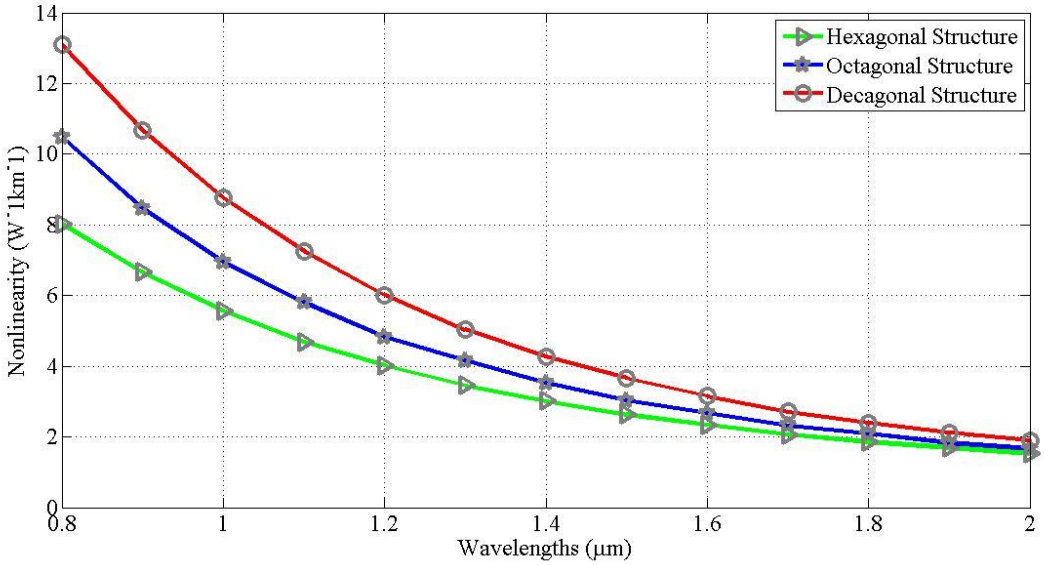

Fig. 4.13: Analysis of nonlinearity against wavelength for three conventional structures.

The plot of nonlinear coefficients of Hy-PCF against wavelengths is shown in Fig. 4.14 along with the plot for D-PCF.

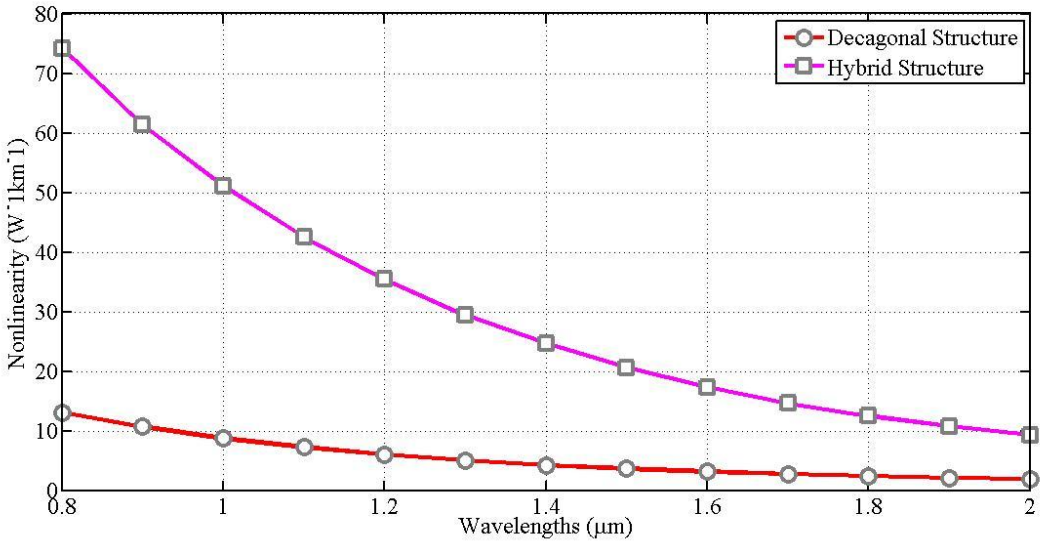

Fig. 4.14: Analysis of nonlinearity against wavelength for hybrid structure.

Since the effective mode area for hybrid structure very small, γ for Hy-PCF is to be more. Moreover γ decreases exponentially with increase in wavelengths. In the Fig. a comparison between the plot of Hy-PCF and D-PCF is seen, from which it is clear that the largest value of nonlinearity is found for this structure. At 0.85 μm the value of γ is 67.54 $W^{-1}km^{-1}$ which is much more compared to that found for the D-PCF. This value is 6 times larger than that of the commercial high nonlinear PCF, and consequently it will have an important application in the nonlinear four-wave mixing (FWM) effect.At 1.55 μm the difference between the values for two structures decreases. At this wavelength, γ for Hy-PCF becomes 19.03$W^{-1}km^{-1}$ only.

4.7 Analysis of Birefringence Against Wavelengths

The values of birefringence are plotted against wavelengths in Fig. 4.15 for the three conventional structures. The values are calculated using equation (2.15). It increases monotonically with increased in wavelengths. In conventional PCFs birefringence is in the order of 10^{-6} only. But the value is little higher for H-PCF compared to the other two. At 0.85 μm birefringence of O-PCF is 0.5×10^{-6} only where birefringence of H-PCF is 4×10^{-6} at that wavelength. At 1.31 μm birefringence of both O-PCF and D-PCF is 2×10^{-6}. But the H-PCF has provided 6×10^{-6} birefringence value.

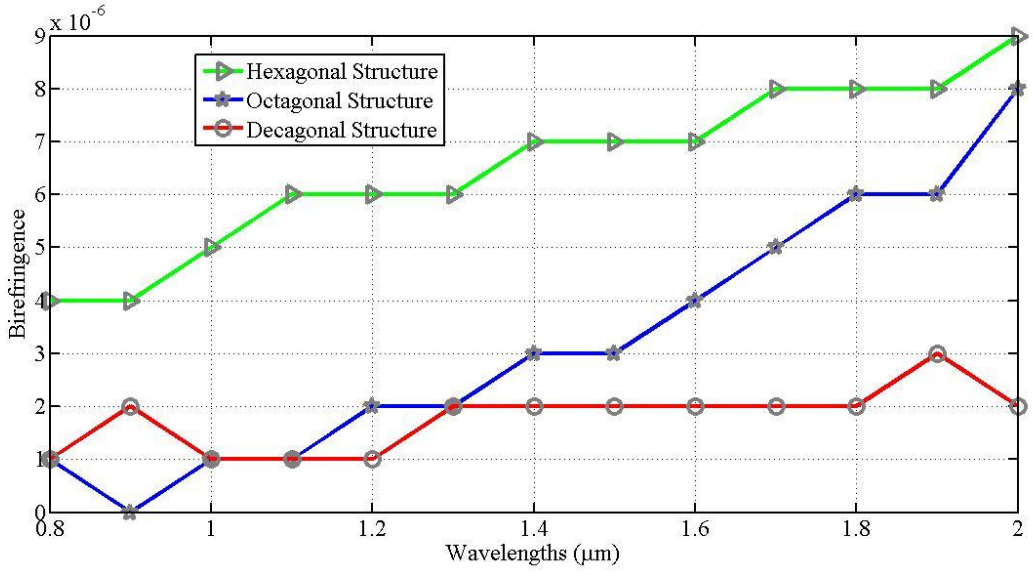

Fig. 4.15: Analysis of birefringence against wavelength for three conventional structures.

From the figure it is also seen that the curves of H-PCF and O-PCF is showing almost linearly increasing pattern whereas the curve of D-PCF is quite flattened in shape.

The birefringence vs. wavelengths plot of Hy-PCF is shown in Fig. 4.16. It is seen that the hybrid structure has provided high birefringence value of the order of 10^{-3}. Introducing asymmetry in the structure and use of elliptical air hole has increased its birefringence. Also a linearly increasing birefringence curve is seen from the figure. At 1.55 μm 4.34×10^{-3} birefringence is obtained by Hy-PCF where only 7×10^{-6} was obtained by H-PCF. Normally birefringence is not a desired property in PCFs, but high birefringence is necessary for polarization maintaining applications. Obviously the Hy-PCF is suitable for this.

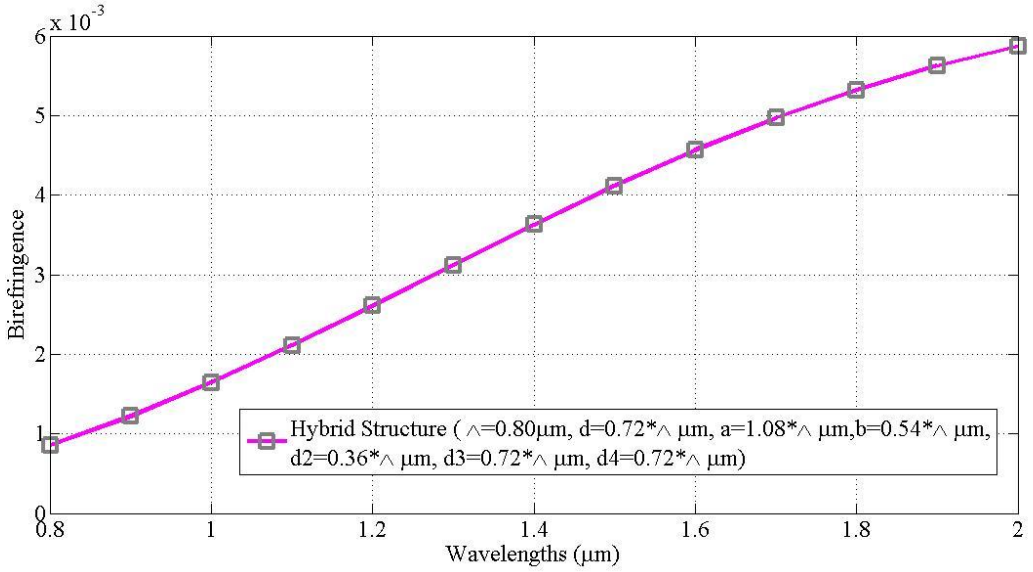

Fig. 4.16: Analysis of birefringence against wavelength for hybrid structure

4.8 Effects of Change in Pitch on Hy-PCF

To ensure feasibility of the design, variations in pitch should not affect the transmission properties much. That's why the tolerance analysis is performed for the Hy-PCF in this thesis.

4.8.1 Effects on Dispersion

The dispersion characteristics of Hy-PCF under optimum parameters is described in Section 4.2, where it is seen that it provides large negative dispersion compared to the conventional PCF structures.

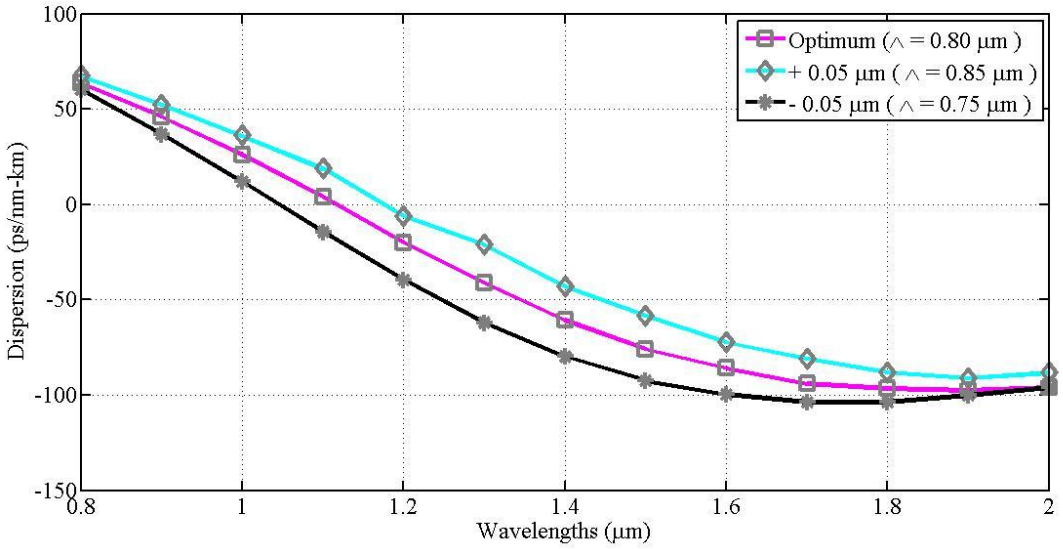

Fig. 4.17: Variation of dispersion characteristics of Hy-PCF under pitch change.

The most appreciable result was found for the third optical window where at 1.55 μm −81.08 ps/km-nm dispersion is obtained. Also the dispersion curve becomes almost flattened afterwards, which is much desired. In Fig. 4.17, for +/− 0.05 μm (6.25%) change in pitch, variation on the dispersion profile is shown. It is seen from the Fig. that when pitch is increased dispersion has increased and when pitch is decreased, dispersion has decreased. But no abrupt change is seen among the curves.

At 0.85 μm 54.5 ps/km-nm dispersion was found for the optimum pitch (0.80 μm) whereas 59 ps/km-nm is found for Λ= 0.85 μm and 48 ps/km-nm is found for Λ= 0.75 μm. Therefore only about +/− 4 ps/km-nm change has appeared for 0.05 μm change in pitch. For 1.31 μm +/− 20 ps/km-nm change from the optimum value is found with −23.34 ps/km-nm dispersion value for Λ= 0.85 μm, −63.4 ps/km-nm dispersion value for Λ= 0.75 μm. But at the most desired wavelength of 1.55 μm, change decreases to −15 ps/km-nm. At this wavelength −65.26 ps/km-nm dispersion is found for Λ= 0.85 μm and −95.96 ps/km-nm

dispersion is found for Λ= 0.75 μm. Indeed, these dispersion variations are acceptable for long haul optical communication.

4.8.2 Effects on Confinement Loss

In Fig. 4.18 change in confinement loss characteristics due to 0.05 μm increase or decrease in pitch is observed.

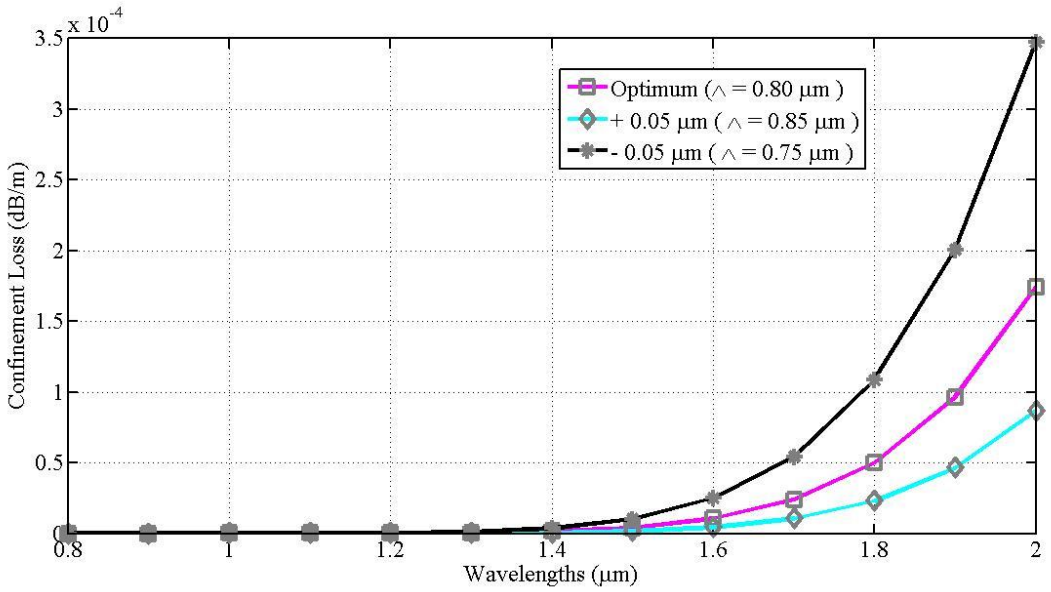

Fig. 4.18: Variation of confinement loss curve of Hy-PCF under pitch change

It is seen from the figure that confinement loss is very sensitive to pitch. The variation increases for large wavelengths. The loss increases with decrease in pitch and decreases with increase in pitch. But the confinement loss value is so small that the variation can be ignored for the wavelengths of first and second optical transmission windows. At 1.55 μm 7.27×10^{-6} dB/m confinement loss was found for optimum pitch. It has changed to 2.96×10^{-6} only for Λ= 0.85 μm but has become 1.75×10^{-5} dB/m for Λ= 0.75 μm. Therefore the confinement loss value is sufficient to be neglected for change in pitch.

4.8.3 Effects on Effective Mode Area

Effective mode area hardly depends on pitch-change in large wavelengths. For the Hy-PCF the change of effective mode area is found very small for 6.25% increase or decrease in pitch. In Fig. 4.19 the effects on effective mode area for pitch-change is shown. It is seen

that at 0.85 μm wavelengths A_{eff} is 2.75 μm^2 for optimum pitch. It has become 3 μm^2 for Λ= 0.85 μm and 2.53 μm^2 for Λ= 0.75 μm. So the change is only +/− 0.25 μm^2 which can be ignored. With increase in wavelengths this variation becomes more negligible. At 1.55 μm, the values obtained for Λ= 0.85 μm, 0.80 μm and 0.75 μm is 5.53 μm^2, 5.43 μm^2 and 5.3 μm^2 respectively.

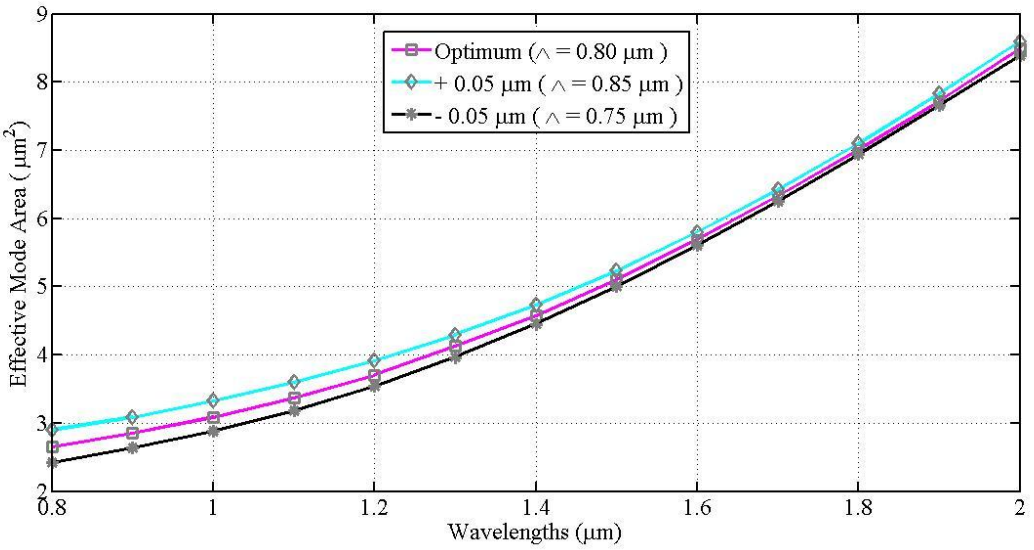

Fig. 4.19: Variation of effective mode area of Hy-PCF under pitch change

4.8.4 Effects on Nonlinearity

Behavior of nonlinear coefficient (γ) on changing pitch value 6.25% is shown in Fig. 4.20. γ is inversely proportional with A_{eff} when value of nonlinear coefficient is constant. Therefore comparing Fig. 4.20 with Fig. 4.19 it is seen as well.Unlike A_{eff}, γ increases with decrease in pitch and vice versa. The variation is comparatively more at smaller wavelengths. At 0.85 μm only +/−5 $W^{-1}km^{-1}$change is found. At that wavelength, 73 $W^{-1}km^{-1}$ γ is obtained for Λ= 0.75 μm, 67.62 $W^{-1}km^{-1}$ γ is obtained for Λ= 0.80 μm (optimum pitch) and 62.06 $W^{-1}km^{-1}$ γ is obtained for Λ= 0.85 μm. The difference becomes only +/−1.3$W^{-1}km^{-1}$ for 1.31 μm wavelengths. After 1.50 μm, no change in γ has appeared for pitch variation. This implies that the highly appreciable result is found for the most desired wavelengths region of optical communication field. Moreover the value is less than 20$W^{-1}km^{-1}$ which is acceptable for being similar to that of the commercial high nonlinear PCF.

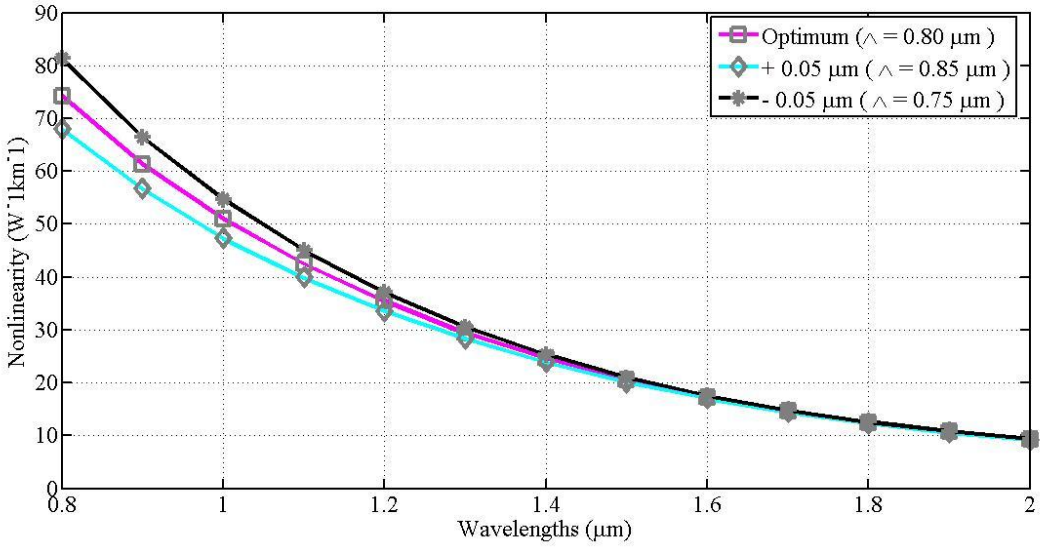

Fig. 4.20: Variation of effective mode area of Hy-PCF under pitch change

4.8.5 Effects on Birefringence

The impact of 6.25% pitch-change on birefringence of the Hy-PCF is shown in Fig. 4.21.

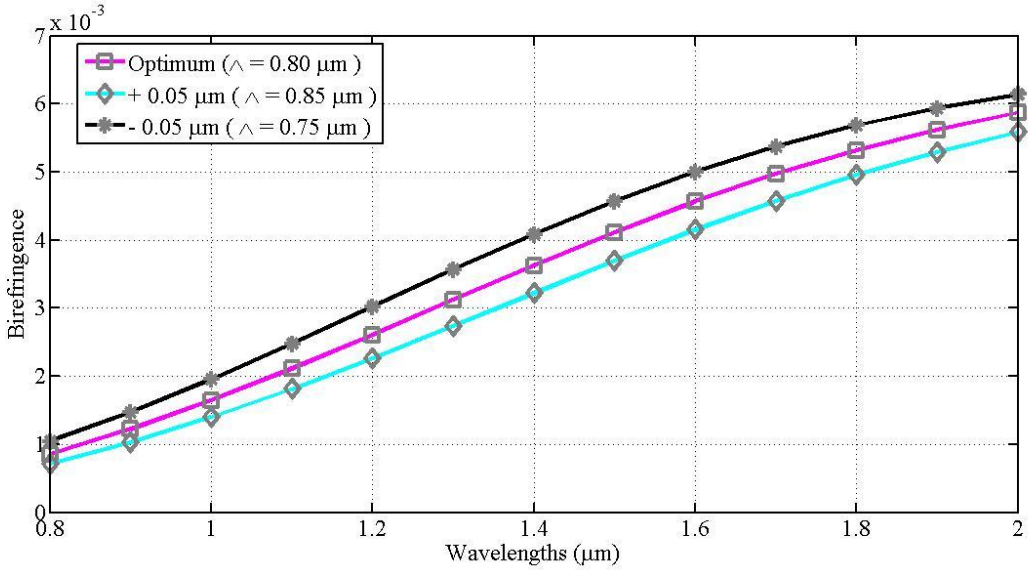

Fig. 4.21: Variation of birefringence of Hy-PCF under pitch change

It is seen that birefringence increases with decrease in pitch value. Only about 9.2% changes in birefringence is found for 0.05 μm increase or decrease in pitch. Variation is

more in large wavelengths. At 1.55 μm 4.34×10^{-3} birefringence is obtained for optimum pitch, whereas 4.8×10^{-3} birefringence is found for $\Lambda = 0.75\mu m$. For $\Lambda = 0.85\mu m$ the value decreases to 3.95×10^{-3}. Therefore these changes are not so large to be counted as a violation of tolerance limit.

4.9 Conclusion

The overall analysis of the comparison shows that each structure has respective advantages and drawbacks over each other. The best structure can be chosen based on the required applications.

CHAPTER 5

CONCLUSION AND FUTURE WORKS

5.1 Introduction

In this final chapter, we have summarized the out-come of our intended research work to fulfill the desired objectives. Here, we have also tried to provide suggestions for future work.

5.2 Conclusion

In this thesis, a comparison among different PCF structures is carried out to analyze their performance over various transmission properties. The numerical analysis along with design description of each model is provided. The finite element method (FEM) has been applied to carry out the modal solution of the PCFs. COMSOL Multi-physics 4.4 Simulation Software has been employed as modeling tool.

The analysis shows that the effective mode index, dispersion, confinement loss, effective mode area, nonlinear coefficients and birefringence property of PCF depends largely on the geometrical shape of the structure. In this work a hexagonal, an octagonal, and a decagonal PCF model are designed with same number of air hole rings, air hole diameter, pitch, core-cladding materials and their properties are compared. Also a hybrid PCF structure is designed with same number of air hole rings and compared with those models. The hexagonal, octagonal and decagonal shaped PCFs have shown near to zero dispersion properties along with very negligible confinement loss, large effective mode area and negligible birefringence whereas the Hy-PCF has provided more negative dispersion with low loss, small effective mode area and high birefringence.

It is found that the effective mode index (η_{eff}) decreases with the increase in wavelength which is in good agreement with the published research papers [4], [10], [13] and [14]. For the change in geometrical shape this nature remains unchanged but different values are obtained. The lowest value of η_{eff} is obtained for Hy-PCF. Next higher value is shown by

D-PCF and finally H-PCF has shown the highest mode index value. η_{eff} decreases more rapidly with increase in wavelengths for Hy-PCF than the conventional structures.

The dispersion curves of O-PCF, D-PCF and Hy-PCF have decreased almost linearly with increasing wavelengths but the curve of H-PCF has shown variations. At 1.55 μm wavelengths, the calculated dispersion for H-PCF, O-PCF, D-PCF and Hy-PCF are −2.80 ps/nm-km, −8.61 ps/nm-km, −11 ps/nm-km and −81.08 ps/nm-km respectively. These values are better than the relevant values found in [9-12].The introduction of hybrid structure has provided more negative dispersion than that for the conventional structures. Thus it can be said that the hybrid structure is more suitable for dispersion compensation technique where the conventional structures are suitable for obtaining near to zero dispersion value.

The analysis of confinement loss has shown that the D-PCF can give confinement loss in the order of 10^{-9} only which is the lowest among all the described structures. Further the confinement loss of O-PCF is in the order of 10^{-8} and H-PCF is in the order of 10^{-6}.The maximum loss values given by the D-PCF and O-PCF are 7.927×10^{-9}dB/m and 8.671×10^{-8} dB/m respectively. These values are much lower than the previous designs suggested in [4-6], [8], [12], [13] and [15]. Further the maximum confinement loss found from the analysis of H-PCF is 1.983×10^{-6} dB/m only and is better than loss of [13]. The hybrid PCF has given the highest loss value with order of 10^{-4}(maximum 1.586×10^{-4} dB/m) but this value can be ignored reviewing its other benefits.

At 1.55μm wavelengths the H-PCF, O-PCF and D-PCF have provided 25.42 μm^2, 19.83 μm^2 and 15.7 μm^2 effective mode areas respectively, whereas in case of the hybrid structure the value is much small with maximum 8.503 μm^2 only. The large effective area helps to reduce the effect of non-linear impairments on different PCF structures. Consequently the value of nonlinear coefficient is very small in H-PCF, O-PCF and D-PCF compared to the large value of Hy-PCF. Moreover for three conventional structures of similar parameters the values of nonlinear coefficient are found close to each other ($3.43W^{-1}km^{-1}$, $2.865W^{-1}km^{-1}$ and $2.493\ W^{-1}km^{-1}$ respectively at 1.55 μm).At 0.85 μm the value of γ for Hy-PCF is found 6 times larger ($67.54\ W^{-1}km^{-1}$) than that of the commercial high nonlinear PCF which can be useful for the application in the nonlinear four-wave mixing (FWM) effect.

In conventional PCF structures the birefringence is found very negligible with order of 10^{-6} only. But the value is higher for Hy-PCF where asymmetry is introduced in the structure. At 1.55 μm 4.34×10^{-3} birefringence is obtained by Hy-PCF where only 7×10^{-6} is obtained by H-PCF. The high birefringence has made the Hy-PCF suitable for polarization maintaining applications.

To ensure the design flexibility of the modified design (Hybrid) the tolerance analysis is performed for the Hy-PCF by varying its pitch. It has been observed that no abrupt change is seen in the results.

5.2 Suggestions for Future Works

- In this work the comparison of different structures has been performed for chromatic dispersion, confinement loss, effective mode area, nonlinear coefficient and birefringence. Further study can be carried out considering dispersion due to polarization effect, leakage loss, bend loss, splice loss, effective V-parameter, numerical aperture etc.
- Instead of using pure silica, doped material for the core and cladding can be used to study the performance of the designed structures.
- Further study can be carried out to compare the properties of designed PCF with conventional single mode optical fiber.

REFERENCES

[1] J. M. senior, Optical Fiber Communications, Principles and Practice, 3rd Edition, Pearson, 2009.

[2] G. P. Agrawal, Fiber Optic Communication Systems, 3rd edition, Wiley, 2002.

[3] Gerd Keiser, Optical Fiber Communications, 2nd edition, McGraw Hill, 1991.

[4] M. M. Haque, M. S. Rahman, M. Samiul Habib, M. Selim Habib, S. M. A. Razzak, "A New Circular Photonic Crystal Fiber for Effective Dispersion Compensation over E to L Wavelength Bands", Journal of Microwaves and Optoelectronics, Vol. 12, No. 2, pp. 44-54, 2013.

[5] K. Saitoh, M. Koshiba, "Chromatic Dispersion Control in Photonic Crystal Fibers: Application to Ultra-flattened Dispersion", Opt. Express, Vol. 11, No. 8, pp. 843-852, 21 April, 2003.

[6] D. K. Prajapati, R. Bharti, "Dispersion analysis of a Hybrid Photonic Crystal Fiber", International Journal of Recent Research and Review, Vol. VII, Issue 2, June, 2014

[7] S. K. Varshney, N. J. Florous, K. Saitoh, M. Koshiba, and T. Fujisawa, "Numerical Investigation and Optimization of a Photonic Crystal fiber for Simultaneous Dispersion Compensation over S + C + L Wavelength Bands", Optical Communication., Vol. 274, No. 1, pp. 74–79, 2007.

[8] M. A. Shobug, E. Khandker, "Large Negative Dispersion Ultra Flattened Hybrid Photonic Crystal Fiber For Residual Dispersion Compensation over 750 nm Bandwidth", Journal of Multidisciplinary Engineering Science and Technology (JMEST), Vol. 3, Issue 10, October, 2016.

[9] Lukman V, J. M. Cherian, "Design of Highly Birefringent and Low Confinement Loss Photonic Crystal Fibre by Introducing Asymmetric Defect Structures", International Journal of Computer Applications, Vol. 44, No. 20, April 2012.

[10] W. Zhang, Shu-guang Li, Guo-Wen An, Zhen-Kai Fan, Ya-Jie Bao, "Double-cladding Rectangular-lattice Birefringence Photonic Crystal Fiber With Elliptical Air Holes", Opt Quant Electron, Vol. 47, pp. 2649–2657, 2015.

[11] S. Olyaee, F. Taghipour, "Ultra-flattened Dispersion Hexagonal Photonic Crystal Fibre with Low Confinement Loss and Large Effective Area", IET Optoelectronics, Vol. 6, pp. 82-87, April 2012.

[12] S.M.A. Razzak, Y. Namihira, "Theoretical Design of a Large Effective Mode Area Microstructure Optical Fiber", Optica Applicata, Vol. XL, No. 3, 2010.

[13] S. Olyaee and F. Taghipour, "A New Design of Photonic Crystal Fiber with Ultra-flattened Dispersion to Simultaneously Minimize the Dispersion and Confinement Loss", 3rd International Photonics & Opto Electronics Meetings (POEM), 2010.

[14] S. Revathi, S. R. Inbathini, and R. A. Saifudeen, "Highly Nonlinear and Birefringent Spiral Photonic Crystal Fiber", Advances in Optoelectronics. Vol. 2014, pp. 1-6, June, 2014.

[15] S. Olyaee and F. Taghipour, "Design of New Square-lattice Photonic Crystal Fibers for Optical Communication Applications", International Journal of the Physical Sciences Vol. 6 (18), pp. 4405 - 4411, 9 September, 2011.

[16] G. Morthier and P. Vankwikelberge, Handbook of Distributed Feedback Laser Diodes, Artech House, Norwood, MA, 1995.

APPENDIX 1

MATLAB CODES

Sample code for measuring Effective Mode Index

```
clc;
clear all;
close all;

lamda=(0.80:0.1:2.00)

hexa=[1.442575
      1.441914
      1.441234
      1.440543
      1.439848
      1.439154
      1.438459
      1.437784
      1.437111
      1.436447
      1.435792
      1.435146
      1.434499];

octa=[1.442017
      1.441233
      1.440428
      1.439614
      1.4388
      1.437992
      1.437196
      1.436414
      1.435648
      1.434899
      1.434166
      1.433448
      1.432746];

deca=[1.44158
      1.440686
      1.439763
      1.438828
      1.437892
      1.436965
      1.436052
      1.435158
      1.434286
      1.433435
      1.432606
```

```
       1.431798
       1.43101];

plot(lamda,hex,'g->',...
'LineWidth',2,...
'MarkerSize',10,...
'MarkerEdgeColor',[0.5,0.5,0.5])

Hold on
plot(lamda,octa,'b-p',...
'LineWidth',2,...
'MarkerSize',10,...
'MarkerEdgeColor',[0.5,0.5,0.5])

Hold on
plot(lamda,deca,'r-o',...
'LineWidth',2,...
'MarkerSize',10,...
'MarkerEdgeColor',[0.5,0.5,0.5])
legend('Hexagonal Structure','OctagonalStructure','Decagonal Structure')
grid on
xlabel ('Wavelengths (\mum)');
ylabel ('Effective Mode Index');
```

Sample code for measuring Dispersion Coefficient

```
clc;
clear all;
close all;
%HEXAGONAL STRUCTURE
Eta102=[1.442575
      1.441914
      1.441234
      1.440543
      1.439848
      1.439154
      1.438459
      1.437784
      1.437111
      1.436447
      1.435792
      1.435146
      1.434499];
      ita2=Eta102';
lamb2=0.8:.1:2.00;
del2=.1;
for j=2:length(ita2)-1
dd12(j)=(ita2(j-1)-2*ita2(j)+ita2(j+1))/(del2)^2;
end
 dd12=dd12*10^12;
 lambda2=lamb2(2:end-1);
 dd2=dd12(2:end);

for b=1:length(lambda2)
```

```
dd2(b)= -dd2(b)*(lambda2(b)/(3e8));
end
 lambda12=(0.8:.005:2.00);

 ddd2=interp1(lambda2,dd2,lambda12,'cubic');

plot(lambda12(1:20:end),ddd2(1:20:end),'g->',...
'LineWidth',2,...
'MarkerSize',10,...
'MarkerEdgeColor',[0.5,0.5,0.5]);
hold on

%OCTAGONAL STRUCTURE
Eta101=[1.442017
      1.441233
      1.440428
      1.439614
      1.4388
      1.437992
      1.437196
      1.436414
      1.435648
      1.434899
      1.434166
      1.433448
      1.432746];
      ita1=Eta101';
lamb1=0.8:.1:2.00;
 del1=.1;
fori=2:length(ita1)-1
  dd1(i)=(ita1(i-1)-2*ita1(i)+ita1(i+1))/(del1)^2;
end

 dd1=dd1*10^12;
lambda=lamb1(2:end-1);
dd=dd1(2:end);

for a=1:length(lambda)
dd(a)= -dd(a)*(lambda(a)/(3e8));
end
lambda1=(0.8:.005:2.00);

ddd=interp1(lambda,dd,lambda1,'cubic');
plot(lambda1(1:20:end),ddd(1:20:end),'b-p',...
'LineWidth',2,...
'MarkerSize',10,...
'MarkerEdgeColor',[0.5,0.5,0.5])
hold on

%DECAGONAL STRUCTURE
Eta103=[1.44158
      1.440686
      1.439763
      1.438828
      1.437892
      1.436965
```

```
      1.436052
      1.435158
      1.434286
      1.433435
      1.432606
      1.431798
      1.43101];

      ita3=Eta103';
lamb3=0.8:.1:2.00;
 del3=.1;
for k=2:length(ita3)-1
dd13(k)=(ita3(k-1)-2*ita3(k)+ita3(k+1))/(del3)^2;
end

 dd13=dd13*10^12;
 lambda3=lamb3(2:end-1);
 dd3=dd13(2:end);

for c=1:length(lambda3)
          dd3(c)= -dd3(c)*(lambda3(c)/(3e8));
end
 lambda13=(0.8:.005:2.00);

 ddd3=interp1(lambda3,dd3,lambda13,'cubic');
plot(lambda13(1:20:end),ddd3(1:20:end),'r-o',...
'LineWidth',2,...
'MarkerSize',10,...
'MarkerEdgeColor',[0.5,0.5,0.5]);

grid on
legend('Hexagonal Structure','Octagonal Structure','Decagonal Structure')
xlabel('Wavelengths (\mum)');
ylabel('Dispersion (ps/nm-km)');
```

Sample Code for measuring Confinement Loss

```
clc;
clear all;
close all;
lamda=(1.5:0.1:2.00)*10^(-6);
lamda1=(1.5:0.1:2.00);
%HEXA
neffh=[-3.688491  -5.670307  -8.610844 -12.91568 -13.88942 -
17.07242]*10^(-8);
l=length(lamda);
lossh=1:l;
fori=1:1:l
lossh(i)=((40*pi)/(log((10)*lamda(i))))*neffh(i);
end
plot(lamda1,lossh,'g->',...
'LineWidth',2,...
'MarkerSize',10,...
'MarkerEdgeColor',[0.5,0.5,0.5])
```

```
hold on
grid on
%OCTA
neffo=[-0.201837 -0.4561907 -0.9819906 -2.016951 -3.962363 -
7.465439]*10^(-9);
l=length(lamda);
losso=1:l;
fori=1:1:l
losso(i)=((40*pi)/(log((10)*lamda(i))))*neffo(i);
end
plot(lamda1,losso,'b-p',...
'LineWidth',2,...
'MarkerSize',10,...
'MarkerEdgeColor',[0.5,0.5,0.5])
hold on
grid on
%DECA
neffd=[0 0 -1.928986 -2.992117 -4.557781 -6.825277]*10^(-10);
l=length(lamda);
lossd=1:l;
fori=1:1:l
lossd(i)=((40*pi)/(log((10)*lamda(i))))*neffd(i)
end
plot(lamda1,lossd,'r-o',...
'LineWidth',2,...
'MarkerSize',10,...
'MarkerEdgeColor',[0.5,0.5,0.5])
hold on
grid on
legend('Hexagonal Structure','Octagonal Structure','Decagonal Structure')
xlabel ('Wavelengths (\mum)');
ylabel ('Confinement Loss (dB/m)');
```

Sample Code for measuring Effective Area

```
clc;
clear all;
close all;
lamda=(0.80:0.1:2.00);

%Hexagonal
Y1= [2.84E-07
2.46E-07
2.20E-07
2.02E-07
1.88E-07
1.78E-07
1.70E-07
1.65E-07
1.60E-07
1.57E-07
1.54E-07
1.51E-07
1.47E-07];
```

```
Y2= [0.003289
0.002303
0.001711
0.001333
0.00108
9.04E-04
7.74E-04
6.81E-04
6.07E-04
5.49E-04
5.03E-04
4.64E-04
4.18E-04];
hex=((Y1.^2)./Y2).*10^12;

plot(lamda,hex,'g->',...
'LineWidth',2,...
'MarkerSize',10,...
'MarkerEdgeColor',[0.5,0.5,0.5])
holdon

%Octagonal
Y1= [1.63E-07
1.43E-07
1.29E-07
1.19E-07
1.13E-07
1.08E-07
1.06E-07
1.05E-07
1.04E-07
1.05E-07
1.05E-07
1.07E-07
1.08E-07];

Y2= [0.001414
9.89E-04
7.34E-04
5.74E-04
4.70E-04
4.00E-04
3.52E-04
3.18E-04
2.93E-04
2.76E-04
2.63E-04
2.53E-04
2.46E-04];

octa=((Y1.^2)./Y2).*10^12;
plot(lamda,octa,'b-p',...
'LineWidth',2,...
'MarkerSize',10,...
'MarkerEdgeColor',[0.5,0.5,0.5])
hold on
```

```
%Decagonal
Y1= [2.96E-07
2.51E-07
2.20E-07
1.98E-07
1.83E-07
1.72E-07
1.64E-07
1.58E-07
1.54E-07
1.52E-07
1.50E-07
1.49E-07
1.48E-07];

Y2= [0.005831
0.003843
0.002692
0.001986
0.001532
0.001228
0.001018
8.69E-04
7.59E-04
6.78E-04
6.15E-04
5.66E-04
5.27E-04];
deca=((Y1.^2)./Y2).*10^12

plot(lamda,deca,'r-o',...
'LineWidth',2,...
'MarkerSize',10,...
'MarkerEdgeColor',[0.5,0.5,0.5])
hold on
grid on

%Hybrid
Y1= [8.07E-08
6.71E-08
5.72E-08
4.99E-08
4.43E-08
4.00E-08
3.64E-08
3.35E-08
3.10E-08
2.89E-08
2.70E-08
2.53E-08
2.38E-08];

Y2= [0.002456
0.001578
0.001061
7.39E-04
```

```
5.30E-04
3.88E-04
2.90E-04
2.20E-04
1.69E-04
1.32E-04
1.04E-04
8.29E-05
6.67E-05];
hybrid=((Y1.^2)./Y2).*10^12
plot(lamda,hybrid,'m-s',...
'LineWidth',2,...
'MarkerSize',10,...
'MarkerEdgeColor',[0.5,0.5,0.5])
grid on
 legend('Hexagonal Structure','Octagonal Structure','Decagonal
Structure','Hybrid Structure')
xlabel ('Wavelengths (\mum)');
ylabel ('Effective area ( \mum^2)');
```

Sample Code for measuring Birefringence

```
clc;
clear all;
close all;
lamda=(0.80:0.1:2.00)

hex=[4 4 5 6 6 6 7 7 7 8 8 8 9]*10^(-6);
octa=[1 0 1 1 2 2 3 3 4 5 6 6 8]*10^(-6);
deca=[1 2 1 1 1 2 2 2 2 2 2 3 2]*10^(-6);

plot(lamda,hex,'g->',...
'LineWidth',2,...
'MarkerSize',10,...
'MarkerEdgeColor',[0.5,0.5,0.5])
holdon
plot(lamda,octa,'b-p',...
'LineWidth',2,...
'MarkerSize',10,...
'MarkerEdgeColor',[0.5,0.5,0.5])
holdon
plot(lamda,deca,'r-o',...
'LineWidth',2,...
'MarkerSize',10,...
'MarkerEdgeColor',[0.5,0.5,0.5])

grid on
legend('Hexagonal Structure','Octagonal Structure','Decagonal Structure')
xlabel ('Wavelengths (\mum)');
ylabel ('Birefringence');
```

Sample Code for measuring Nonlinearity

```
clc;
clear all;
close all;

hAeff=[24.5230
   26.2770
   28.2876
   30.6107
   32.7259
   35.0487
   37.3385
   39.9780
   42.1746
   44.8980
   47.1491
   49.1401
   51.6962];
oAeff=[18.7900
   20.6764
   22.6717
   24.6707
   27.1681
   29.1600
   31.9205
   34.6698
   36.9147
   39.9457
   41.9202
   45.2530
   47.4146];
dAeff=[15.0259
   16.3937
   17.9792
   19.7402
   21.8597
   24.0912
   26.4204
   28.7273
   31.2464
   34.0767
   36.5854
   39.2244
   41.5636];

L= (0.80:0.1:2.00)*10^-6;
w= (0.80:0.1:2.00);

%hexagonal
for i=1: length(L)
n2=2.507*10^-8;
Yh(i)= (2*pi*n2)/(L(i)*hAeff(i))*10^3;
end
plot(w,Yh, 'g->',...
'LineWidth',2,...
```

```
'MarkerSize',10,...
'MarkerEdgeColor',[0.5,0.5,0.5]);
hold on
grid on

%octagonal
for i=1: length(L)
n2=2.507*10^-8;
Yo(i)= (2*pi*n2)/(L(i)*oAeff(i))*10^3;
end
plot(w,Yo, 'b-p',...
'LineWidth',2,...
'MarkerSize',10,...
'MarkerEdgeColor',[0.5,0.5,0.5]);
hold on
grid on

%decagonal
for i=1: length(L)
n2=2.507*10^-8;
Yd(i)= (2*pi*n2)/(L(i)*dAeff(i))*10^3;
end
plot(w,Yd, 'r-o',...
'LineWidth',2,...
'MarkerSize',10,...
'MarkerEdgeColor',[0.5,0.5,0.5]);
hold on
grid on
legend('Hexagonal Structure','Octagonal Structure','Decagonal Structure')
xlabel('Wavelengths (\mum)');
ylabel('Nonlinearity (W ^-1km^-1)');
```